2015 Habitat Monitoring and Assessment: Permafrost Component CD5 Development Project

Aaron F. Wells
Christopher S. Swingley
Matthew J. Macander
Tracy Christopherson

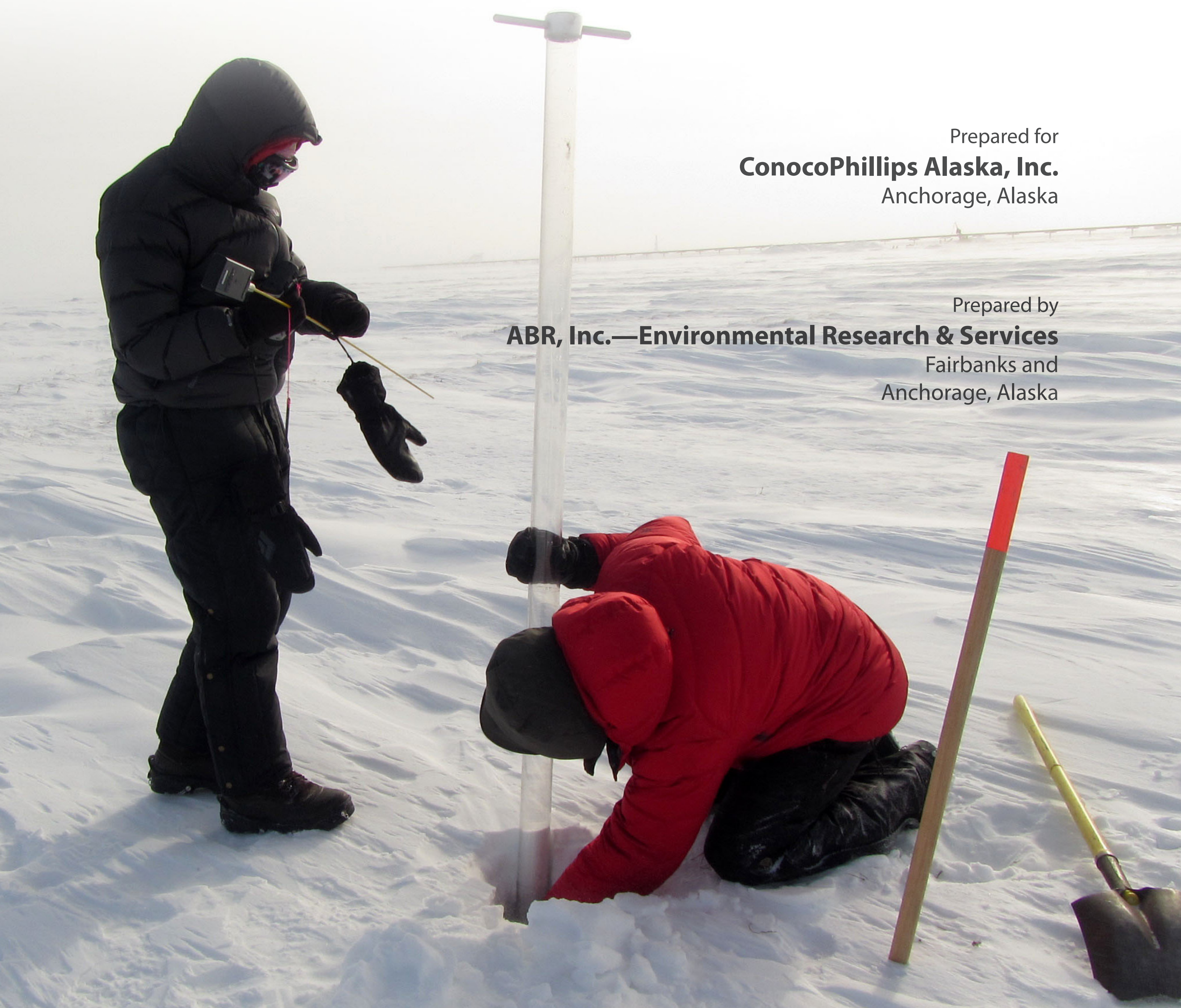

Prepared for
ConocoPhillips Alaska, Inc.
Anchorage, Alaska

Prepared by
ABR, Inc.—Environmental Research & Services
Fairbanks and
Anchorage, Alaska

2015 HABITAT MONITORING AND ASSESSMENT: PERMAFROST COMPONENT

CD5 DEVELOPMENT PROJECT

FINAL REPORT

Prepared for

ConocoPhillips Alaska, Inc.

P.O. Box 100360

Anchorage, AK 99510

Prepared by

Aaron F. Wells

Christopher S. Swingley

Matthew J. Macander

Tracy Christopherson

ABR, Inc.—Environmental Research and Services

P.O. Box 240268

Anchorage, AK 99524

and

P.O. Box 80410

Fairbanks, AK 99708

February 2016

Printed on recycled paper.

EXECUTIVE SUMMARY

This report presents the results of the second year of the soil temperature monitoring component of the CD5 Habitat Monitoring Study. The objectives of the second year were to (1) complete snow surveys at Permafrost Monitoring Plots; (2) analyze, synthesize, and report findings on one complete year of soil temperature data in the CD5 Habitat Monitoring Study Area; and (3) present findings at an agency and stakeholder meeting in February 2016.

Snow surveys were conducted 7–9 April 2015 in the CD5 Habitat Monitoring Study Area to measure end of winter snow depth and density data. Snow survey data was measured and recorded at the 16 soil temperature monitoring stations (i.e., “Hobo Installations”) originally installed at Permafrost Monitoring Plots in September 2013. The Hobo Installations were revisited in August 2015 at which time the soil temperature data were downloaded and the installations removed.

In the office, field data were uploaded to the project database and a series of quality control and quality assurance (QAQC) routines were run on the raw field data using both automated and hand filtering methods. Data were analyzed using a combination of database queries and scripts written in R, a language and environment for statistical computing. Climate data from the Alpine Weather Station, and three nearby National Weather Service stations, were summarized for the monitoring period and compared with long-term (30-year) climate normals. Snow survey data were summarized by Permafrost Monitoring Plot and subarea to determine average depth, density, and Snow water equivalent (SWE). Soil temperature data were analyzed by aggregating the soil temperature data to daily minimum, maximum, mean, standard deviation and median values for each depth and Hobo Installation for two time periods, including the “thaw season” (July 2014–September 2014) and the “freeze season” (October 2014–June 2015), to assess seasonal dynamics in soil temperature. The daily soil temperature data were also grouped by study area to compare the data at a broader spatial scale across the entire July 2014–June 2015 period. Cumulative thawing and freezing n-factors were calculated as the ratio of seasonal degree day sums of the soil at 30 cm depth to the degree days of the air. The cumulative daily thawing and freezing n-factors were calculated for each Hobo Installation and then aggregated by subarea.

Air temperatures at the Alpine Weather Station over the study period ranged from -40.7 °C on 3 March 2015 to 25.9 °C on 20 June 2015. Mean air temperatures for summer 2014 (4.6 °C), winter 2014–2015 (-15.8 °C) and spring 2015 (8.8 °C) at the Alpine Weather Station were very similar to the temperatures reported by the National Weather Service stations. Stations reported slightly colder than normal summer 2014 temperatures, and warmer temperatures in winter 2014–2015 and spring 2015 (3.0 and 3.7 °C warmer than normal, respectively). Precipitation was slightly below normal at the National Weather Service stations in summer 2014 and above normal in winter 2014–2015. Similarly, National Weather Service stations recorded above-normal maximum snow depth for winter 2014–2015.

The mean snow depth at Hobo Installations ranged from 158 to 396 mm, with a mean of 277 mm. Vegetation class appeared to be an important factor influencing snow depth: all of the shallow (≤248 mm) snow plots had Wet Sedge Meadow Tundra vegetation, whereas 75% of the deep (≥322 mm) snow plots had Wet Sedge-Willow Tundra vegetation. Shrub abundance plays a key role in trapping snow in the study area, as even sparse, low-statured shrub vegetation tends to have higher snow-holding capacity than graminoid-dominated tundra. Mean snow density, based on the five snow cores at each plot, ranged from 0.25 to 0.32 g/cm³. Snow depth can be one of the most important factors explaining variation in snow density hence, snow density was modeled as a function of snow depth. The fitted model with snow depth as the predictor explained >30% of the variance in snow density. SWE estimated based on the density model ranged from 53.7 to 102.0 mm. When the data were aggregated to subarea, snow was deepest in the Test Area North subarea (298 mm) and shallowest in the Test Area South subarea (252 mm). Reference Area North and Reference Area South had snow depths of 284 and 286 mm, respectively. Density measurements were similar in all subareas, ranging from 0.27 to 0.28 g/cm³. SWE by the density model method ranged from 69.4 to

85.1 mm, with Test Area North having the highest SWE and Test Area South having the lowest SWE.

Fifteen of the 16 Hobo Installations were flooded during 2015 spring breakup. All 16 Permafrost Monitoring Plots had evidence of water inside the waterproof PVC box and several installations were lightly damaged, flipped upside down, and/or disconnected at the L-joint as the result of spring breakup flooding disturbance. In general, soil temperature patterns during the monitoring period followed the mean air temperature, with a lag time in the response of soil temperatures depending on depth. The mean temperature at 30 cm during the thaw season ranged between 0.70 °C (± 0.56 °C) and 2.76 °C (± 1.38 °C). The mean temperatures at 100 cm during the thaw season were slightly colder than those at 30 cm, ranging from -1.31 °C (± 0.40 °C) to -0.98 °C (± 0.30 °C). The mean temperature at 30 cm during the freeze season ranged between -7.39 °C (± 6.06 °C) and -5.61 °C (± 5.69 °C). The mean temperatures at 100 cm during the freeze season were slightly colder than those at 30 cm ranging from -6.86 °C (± 5.05 °C) to -5.21 °C (± 4.29 °C). In general, we observed that soil temperature was quite responsive to changes in air temperature, particularly at the 30 cm depth. However, soil temperature at any given location and time is influenced by several factors in addition to air temperature, including surface organic thickness, and during the winter months, snow depth. Surface organic layers and snow insulate underlying soils from the atmosphere thus reducing the degree to which air temperature affects soil temperature. For instance, the plot with the thinnest surface organic layer also had the highest variability in 30 cm soil temperatures throughout the year, and 2 of the 3 plots with the deepest snow depths had the warmest mean 100 cm temperatures. N-factors integrate the complex relationships between near surface soil temperature, environmental factors (e.g., snow depth, surface organic thickness), and energy fluxes on an easily calculated numerical scale. Soils that are more insulated from the air by thick surficial organic deposits, snow, or surface water will have a lower n-factor, while the n-factor for soils that are less buffered from the air will be higher. In general, n-factors were more variable between plots during the thawing season than during the freezing season. This suggests that during the thawing season soil temperatures were differentially affected by air temperature due to differences in other environmental factors (e.g., surface organic thickness). During the freezing season, soil temperatures were more evenly affected by air temperature and the effects of other factors, such as snow depth, were less important in determining the pattern of soil temperatures observed between plots.

The aggregated soil temperature time series followed similar soil temperature patterns throughout the year as described for the individual Permafrost Monitoring Plots. Mean annual soil temperatures at 30 cm in the two Reference Areas were similar, ranging between -4.48 °C (± 6.39) at Reference Area North and -4.08 °C (±6.63) at Reference Area South. The mean temperature at 30 cm in Test Area North (-4.55 °C ± 6.48) was slightly colder than the two Reference Areas and Test Area South was the coldest subarea with a mean annual soil temperature at 30 cm of -4.70 °C (± 6.76) at 30 cm. The trend was similar for temperature at 100 cm with the warmest temperatures at Reference Area South, and the coldest at Test Area South. The slightly cooler temperatures in Test Area South may be attributed in part to the thinner cumulative organic thickness in this area (35.6 cm) compared to the other three areas (39.0–48.3 cm), and the thinner late winter snow depth (252 mm) compared to the other three (284–298 mm). Overall, the soil temperatures at 30 and 100 cm in all 4 areas were very similar. Test Area South, Test Area North, and Reference Area North were the most similar in mean annual soil temperature, occurring within approximately ±0.20 °C. Reference Area South was the warmest at both 30 and 100 cm and the most different from the other three, but the differences were still relatively small, ±0.72 °C in the most extreme case.

TABLE OF CONTENTS

LIST OF FIGURES

LIST OF TABLES

LIST OF APPENDICES

ACKNOWLEDGMENTS

This study was funded by ConocoPhillips Alaska, Inc. and was managed by Robyn McGhee. Adam Davis-Turak, Exploration Environmental Coordinator with ConocoPhillips Alaska, Inc., provided valuable information regarding the location of ice pads and roads in the CD5 Habitat Monitoring Study Area. Many thanks to all those at Alpine whose efforts led to a safe and successful field season. Allison Zusi-Cobb provided GIS support and created map figures. Pam Odom produced the report, and Janet Kidd and Gerald "JJ" Frost provided thorough reviews. Many thanks to you all!

INTRODUCTION

BACKGROUND

As a condition of the permit (POA-2005-1576) to develop CD5 in the National Petroleum Reserve—Alaska (NE NPRA) and associated infrastructure on the Colville River Delta (CRD), the U.S. Army Corp of Engineers (USACE) stipulated that ConocoPhillips Alaska, Inc. (CPAI) implement a monitoring plan with an adaptive management strategy (Monitoring Plan). The Monitoring Plan (herein Plan) was developed to monitor changes in site conditions and the efficacy of the mitigation measures developed to minimize impacts to natural resources in the project area (ABR and Baker 2013). The Plan committed CPAI to (1) develop a monitoring program prior to construction; (2) prepare monitoring reports on a variety of monitoring components (see below) for review by key stakeholders; and (3) meet with stakeholders annually to review the monitoring reports and the effectiveness of the mitigation measures developed for the project.

MONITORING PROGRAM GOALS AND OBJECTIVES

After four decades of development activities associated with North Slope wetlands, rivers, and streams, and more than ten years of development on the CRD, impacts resulting from gravel placement on tundra and bridge and culvert construction across rivers and streams are well understood. Those impacts have prompted CPAI operations to implement mitigation measures for the CD5 Project in consultation with federal and state agencies.

The Plan's goal is to monitor changes in site conditions and selected resources and to modify, if appropriate, operational practices to minimize impacts on the hydrologic function of the CRD as a result of road, bridge, and pad construction. As discussed with federal agencies at meetings in 2011, an outline of the Plan and a table summarizing the Plan's monitoring components were provided to the USACE in a letter dated 23 November 2011. Subsequent discussions and correspondence through 30 August 2012 identified the following broad level study components to be included in the Plan:

- habitat monitoring (vegetation, geomorphology, sedimentation, permafrost, weather);
- hydrology monitoring;
- erosion control monitoring;
- culvert monitoring; and
- bridge monitoring (Niġliq and Niġliagvik Bridge).

This report presents the results of the permafrost monitoring associated with the habitat monitoring component (hereafter, CD5 Habitat Monitoring Study) of the overall Plan. As described in the CD5 Monitoring Plan (ABR and Baker 2013), the overall goals of the CD5 Habitat Monitoring Study include (1) determining whether gravel placement associated with construction of the CD5 road alters upstream and/or downstream wildlife habitats; (2) describe baseline conditions by sampling vegetation and habitats in permanent plots (Wells et al. 2014); and (3) monitoring vegetation, wildlife habitat, geomorphology, and sedimentation/erosion to assess changes from baseline conditions through time.

The objectives of the second year of the Permafrost Monitoring Study were to:

- complete snow surveys at Permafrost Monitoring Plots;
- analyze, synthesize, and report findings on one complete year of soil temperature data in the CD5 Habitat Monitoring Study Area; and
- present findings at an agency and stakeholder meeting in February 2016.

CD5 HABITAT MONITORING STUDY AREA

DESCRIPTION

This study focuses on the CD5 Habitat Monitoring Study Area located along the Niġliq Channel in the southwestern portion of the CRD on the North Slope of Alaska (Figures 1 and 2). The Alpine Oil Facilities are located directly east of the CD5 Habitat Monitoring Study Area, and the

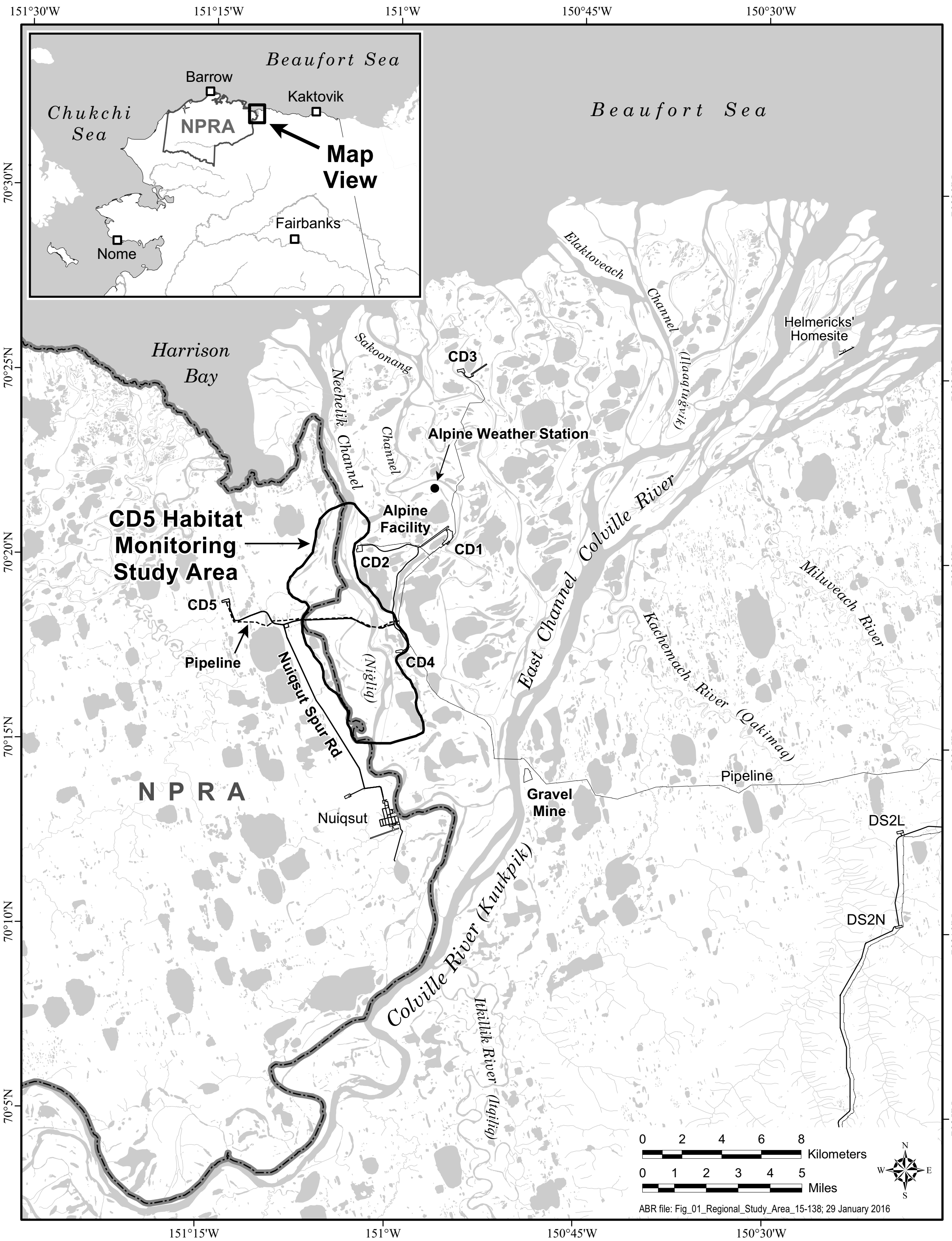

Figure 1. Location of the CD5 Habitat Monitoring Study Area on the Colville River Delta, northern Alaska, 2013–2015.

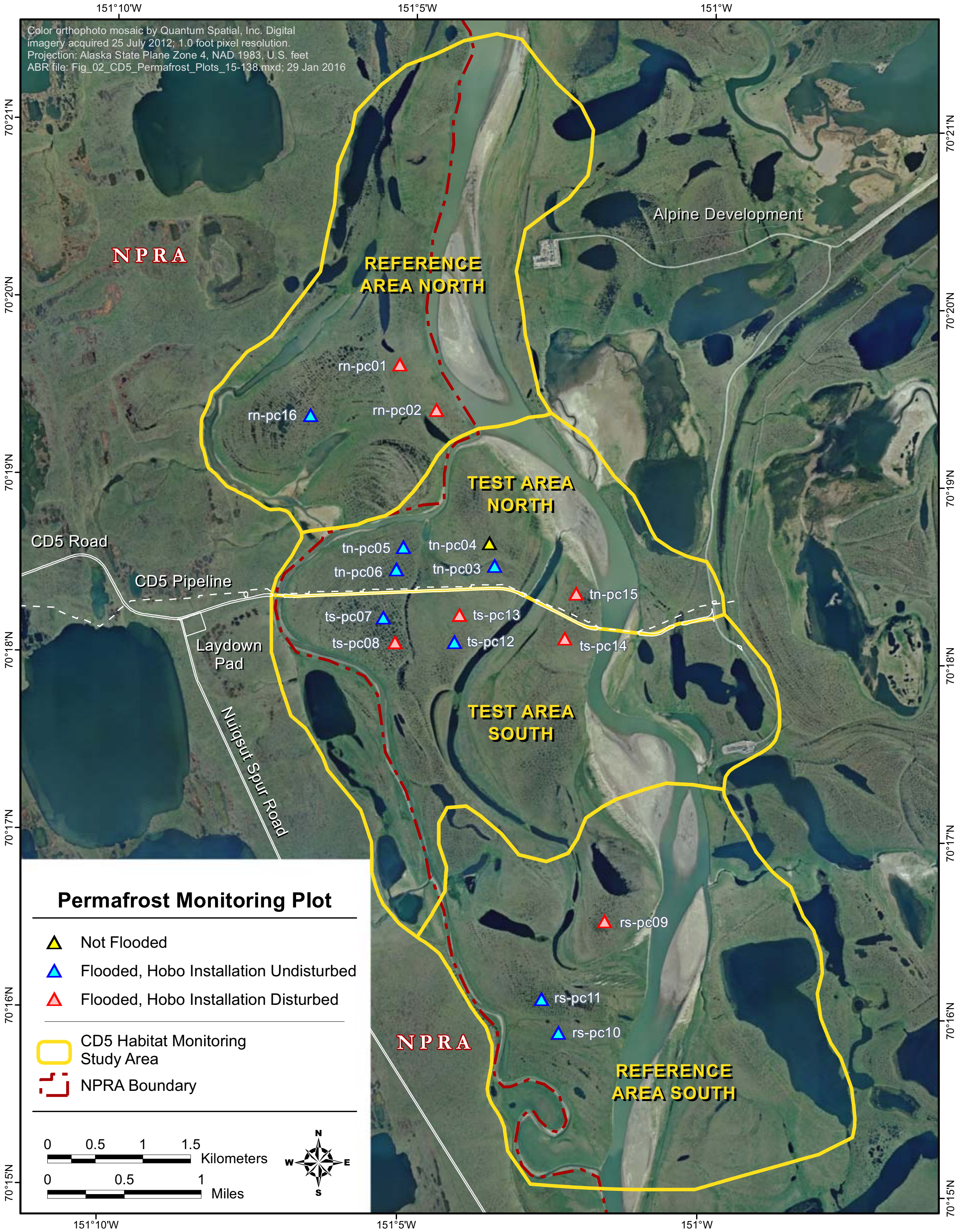

Figure 2. Locations of Permafrost Monitoring Plots with symbology indicating plots at which evidence of 2015 break up flooding was observed, CD5 Habitat Monitoring Study Area, northern Alaska, 2013–2015.

village of Nuiqsut, established in 1971, is located at the head of the CRD several kilometers south of the CD5 Habitat Monitoring Study Area.

The CD5 Habitat Monitoring Study Area has been partitioned into four sub-areas, including test and reference areas (Figure 2). The "test" areas include the areas directly upstream (Test Area South) and downstream (Test Area North) of the proposed CD5 road (ca. 1.9 km long); these areas were predicted by ABR and Baker (2011) to be affected by moderate and high sedimentation and erosion regime changes during a 200 year flood event. The "reference" areas were located approximately 3–5 km upstream (Reference Area South) and downstream (Reference Area North) of the proposed CD5 road and were predicted by ABR and Baker (2011) to be unaffected by the proposed development.

ENVIRONMENT

The Colville River is the largest river on Alaska's North Slope and is one of eight arctic rivers providing significant freshwater discharge to the Arctic Ocean (Walker 1983, Figure 1). The Colville River drains approximately 29% (53,600 km^2) of the North Slope, including most of the foothills (64% of the total Colville River watershed) and smaller areas of the Brooks Range (26%) and coastal plain (10%); Walker 1976. The Colville empties into the Beaufort Sea near the northeastern corner of the National Petroleum Reserve—Alaska (NPRA), midway between Barrow and Kaktovik; the river then slows and forms a delta before it enters the Beaufort Sea. The head of the CRD is located about 3 km downstream of the mouth of the Itkillik River, and 30 km upstream of the Beaufort Sea (Arnborg et al. 1966).

The delta has two main distributaries, the Niġliq (western) Channel and the Colville East Channel (Figure 1). These two channels combined carry about 90% of the water through the delta during spring flooding and 99% during periods of low water (Walker 1983). Smaller channels branching from the Colville East Channel include the Sakoonang, Tamayayak, and Elaktoveach channels.

The CD5 Habitat Monitoring Study Area has a typical arctic maritime climate. Winters are cold and windy and last approximately eight months. Summers are cool and are characterized by low precipitation, overcast skies, fog, and persistent northeast winds. The CD5 Habitat Monitoring Study Area occurs in the zone of continuous permafrost (Jorgenson et al. 2008) and the depth of permafrost is shallow (within 1 m of the soil surface) beneath much of the Study Area, with the exception of active river channels.

FIELD METHODS

CLIMATE MONITORING

The Alpine Weather Station was installed on 10 May 2013 by Polar Alpine, Inc. to monitor weather and climate in the Alpine Development area. The station is located 2.3 km north-northwest of the CD1 facility (Figure 1). The geographical coordinates of the location are N70.36590°, W150.94639° (NAD83). The site elevation is approximately 7.3 m above British Petroleum mean sea level (BPMSL). The Alpine weather station is configured to collect the following data:

- wind speed and direction,
- incoming solar radiation,
- air temperature,
- snow depth,
- precipitation, and
- barometric pressure.

Figure 3 provides an annotated photograph of the weather station's design and instrumentation. Wind speed and direction are measured using an R. M. Young Model 05103-45 Alpine Version Wind Monitor placed 9.25 ft (2.82 m) above the ground. Solar radiation is measured using a Hukseflux LP02 pyranometer with a light spectrum waveband ranging from 305 to 2800 nm. Air temperature is measured using a Lewellen Arctic Research, Inc. Type T Thermocouple. Snow depth is measured using a Campbell Scientific, Inc. Sonic Ranging Sensor SR50A. A Texas Electronics TE525WS Tipping Rain Bucket Rain Gauge with wind screen measures liquid precipitation. Barometric pressure is measured using a Vaisala PTB110 barometer. Full specifications for the Alpine Weather Station instrumentation are provided in Wells et al. (2014). Wind speed and direction, incoming solar radiation, air temperature, and precipitation are recorded at 30-second intervals. Snow depth and

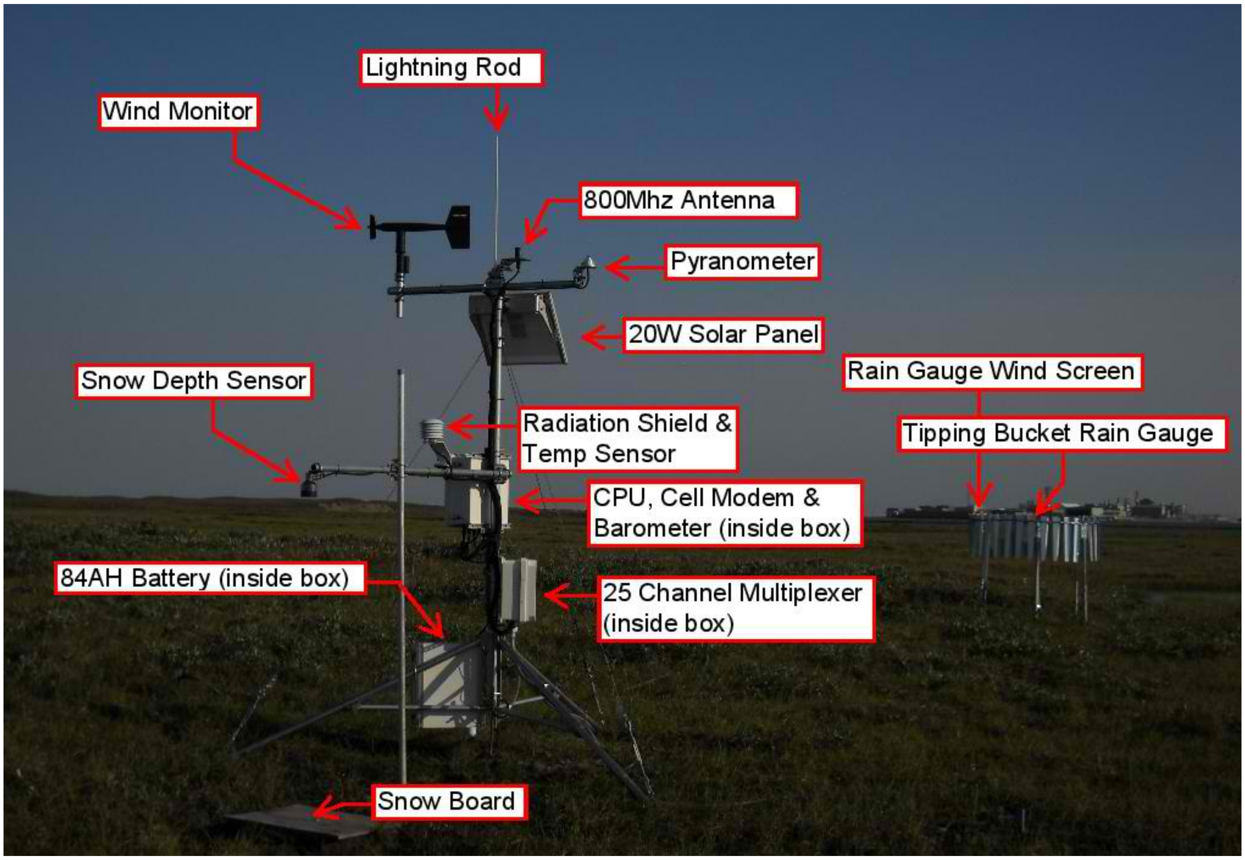

Figure 3. Annotated photograph of the Alpine Weather Station illustrating the station layout and instrumentation, Colville River Delta, northern Alaska, 2013–2015.

barometric pressure are recorded at hourly intervals.

SNOW SURVEYS

Snow survey field methods generally followed Derry et al. (2009), a snow-course measurement protocol developed for the North Slope. That report discussed "snowpack data collection methods as practiced by University of Alaska Fairbanks, Water and Environmental Research Center (WERC) project participants over multiple projects with the intent that these methods serve as a guide for other groups participating in field snow data collection efforts" (Derry et al. 2009).

We measured a snow-course at each Permafrost Monitoring Plot within 10 to 20 m of the Hobo Installation (Figure 4). Plots were accessed in a Hagglund, an all-terrain vehicle designed for travel on snow, following access corridors defined in the tundra travel permit. The Hagglund was parked at least 25 m away from the center of each plot to avoid disturbance before measurement. Snow in arctic tundra environments is more variable in depth than in density (Benson and Sturm, 1993), so a "double sampling" technique was applied, with 60 snow-depth measurements and 5 snow-density measurements recorded per snow-course. Snow depth was measured with a hard, narrow rod graduated in cm. Measurements were recorded on a handheld GPS unit that also stored the location of each measurement. Fifty of the snow-depth measurements were spaced at 1 m intervals in a 25 m by 25 m "L" shaped transect (Figure 5). Each snow-course was oriented with the Hobo Installation between the legs of the "L". Following Derry et al. 2009, the orientation of the legs was "chosen somewhat randomly, but with consideration of snow drift frequency and direction in order to capture natural variability." An additional cluster of ≥10 snow depths was measured around the center of each Hobo Installation to assess whether snow depths there were similar to the snow-course overall.

Snow density was measured by extracting cores with a Snow-Hydro snow sampler (Figure 6) at regular intervals adjacent to each transect (Figure 5), with some effort made to obtain cores that captured the range of depths observed along the snow-course. Similar to the Adirondack sampler used by Derry et al. (2009), the Snow-Hydro sampler has a large inside area (30 cm²) compared to the Standard Federal Sampler, thereby increasing accuracy and reducing error in shallow arctic snowpacks due to the larger sample collected (Woo et al. 1997). Snow density data were recorded in a spreadsheet on a handheld computer; the locations of individual cores were not recorded. We inserted the tube vertically until the ground surface was detected, and recorded the snow depth. Then, we excavated the snow down to the tube/ground interface, covered the bottom of the tube with a gloved hand to prevent loss of snow, inverted the tube and collected the snow sample in a numbered ziploc bag after removing vegetation and other debris. After five cores were collected, the bags were immediately weighed on an electronic scale in the Hagglund.

- Additional data collected at each coring location included:
- thickness of snow in the tube (related to collapse and/or voids in the snowpack);
- thickness of depth hoar (large, low-density, metamorphosed snow crystals that occur at the base of the snowpack) at each core location;
- depth of the largest ice layer at each coring location (if any);
- temperature at the snow/ground interface at each coring location; and
- presence of an ice layer at the bottom of the coring location.

Additional data collected at each plot included:

- azimuth of each transect leg;
- observations of disturbance to the site (if any);
- condition of the soil temperature data logger (if visible);
- photographs along each leg of the transect;
- observations of any vegetation and surface form (e.g., ice-wedge polygon rim) apparent at the site; and
- dominant orientation of any sastrugi (snow ridges that form perpendicular to prevailing wind direction).

SOIL TEMPERATURE MONITORING

A total of 16 soil temperature monitoring stations, herein referred to as “Hobo Installations” were installed at Permafrost Monitoring Plots in the CD5 study area during field surveys between 9–18 September 2013 (Wells et al. 2014). Table 1 provides a cross reference between the study subarea (e.g., Reference Area North), the unique id of each Permafrost Monitoring Plot (i.e., superplot id), the serial number of the Hobo data logger deployed at each associated Hobo Installation, and the dates each Hobo Installation was installed and removed. Cumulative organic thickness, maximum thaw depth, and Alaska Vegetation Classification (AVC) Level IV vegetation classes (Viereck et al. 1992) were measured and recorded at each plot as described in Wells et al. 2014.

Five Hobo Installations were installed in each Test Area, and 3 Hobo Installations were installed in each Reference Area (Figure 2). Each Hobo Installation was equipped with a Hobo U23 Data Logger that includes two permanently attached soil-temperature sensors. The Hobo data loggers were launched according to the manufacturer's instructions using a Hobo U-DTW-1 Waterproof Shuttle prior to fieldwork. Each of the two sensors had a label affixed by the manufacturer identifying them as Channel 1 or Channel 2. Channels 1 and 2 were pre-measured and marked with a marker at 30 cm and 100 cm, respectively, to facilitate placement of each sensor at the appropriate depth. Prior to deployment in the field, each HOBO Data Logger was calibrated in an ice-water bath to within ±0.5°C, and offsets from 0°C were recorded. In the field, each Hobo Data Logger was deployed inside a waterproof box and polyvinyl chloride (PVC) tube system (Figure 7). The loggers were set to record soil temperature once

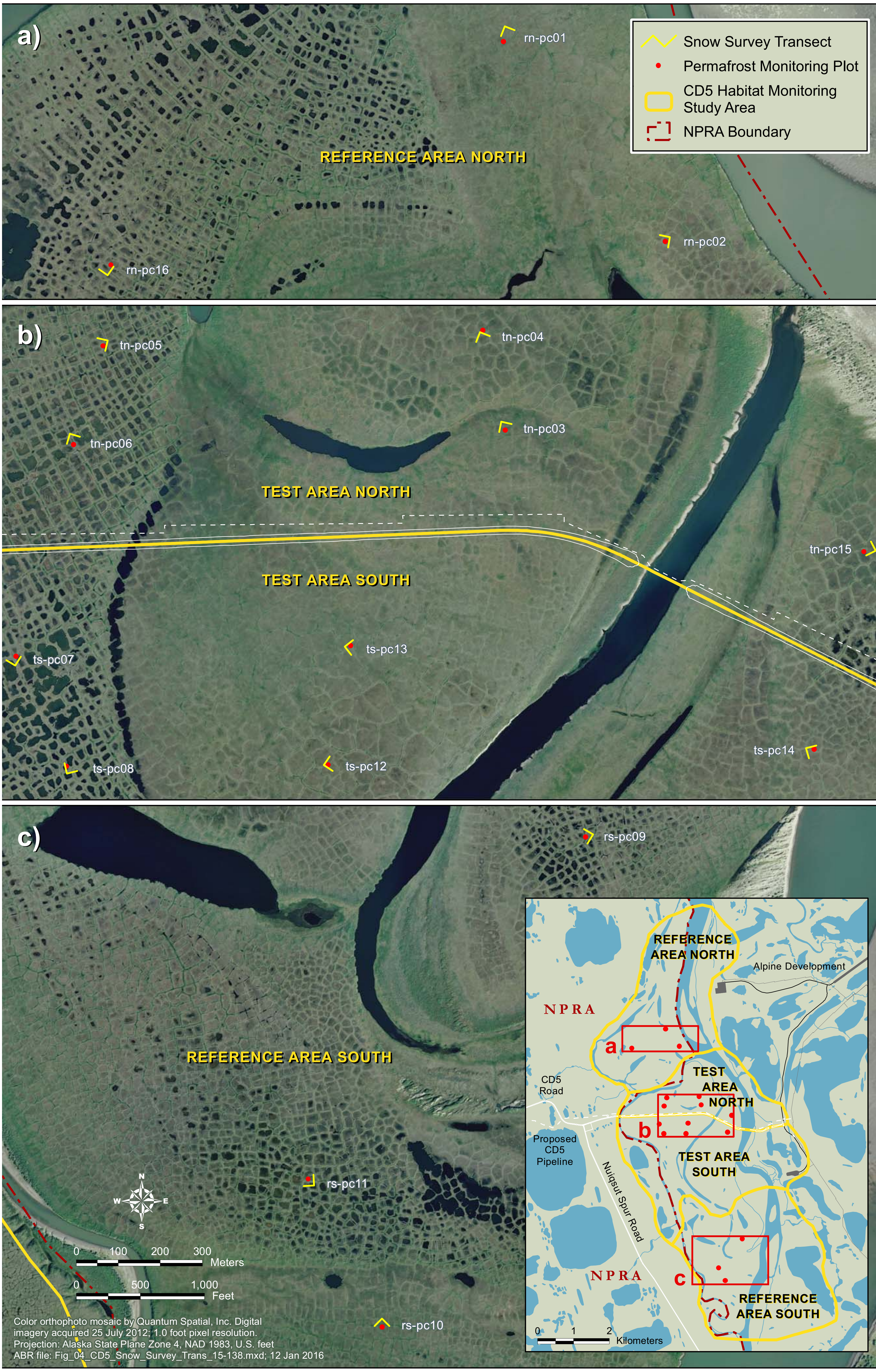

Figure 4. Location and orientation of snow survey transects at each Permafrost Monitoring Plot at each of four subareas, CD5 Habitat Monitoring Study Area, northern Alaska, 2015.

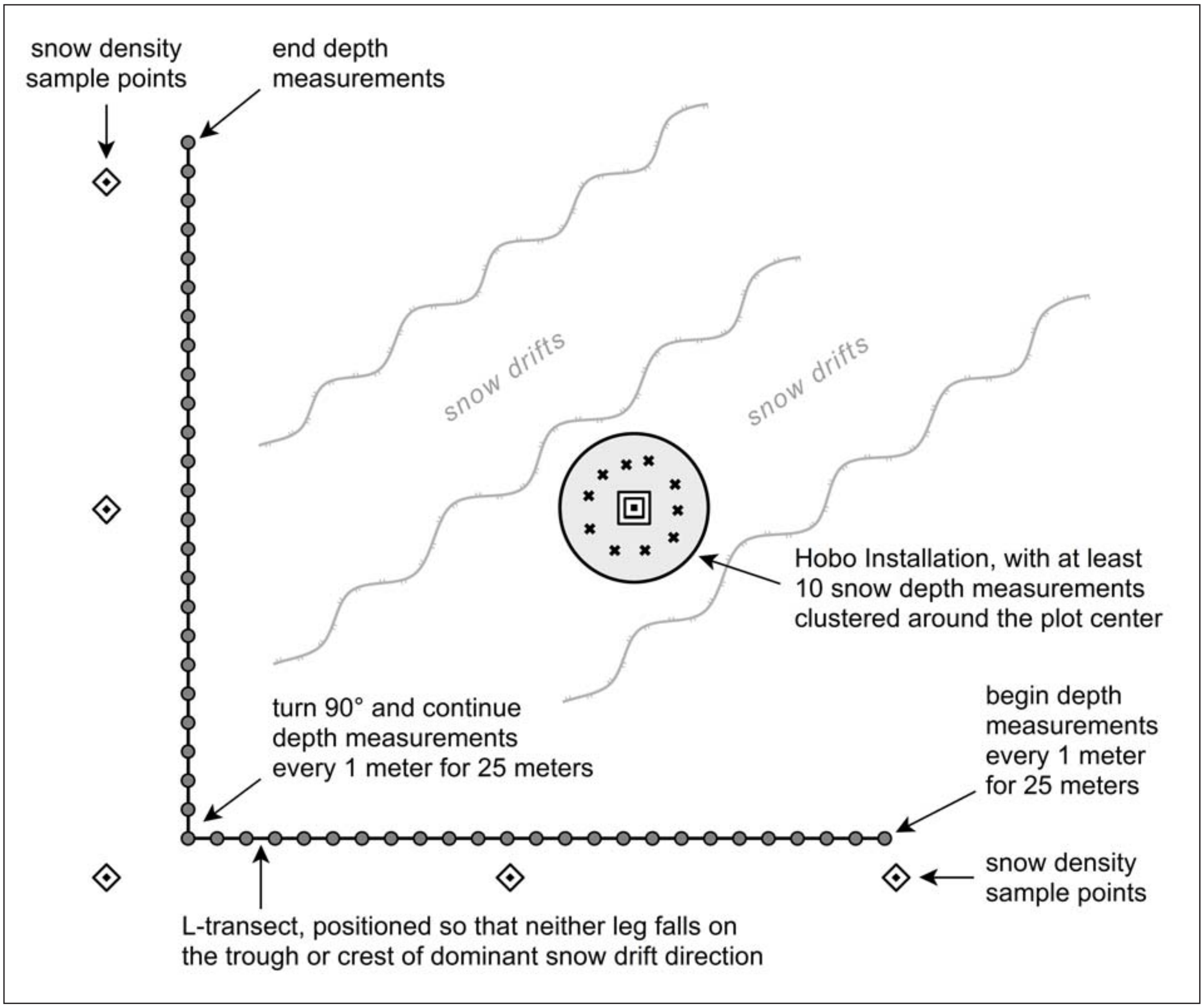

Figure 5. Schematic of snow survey plot design, CD5 Habitat Monitoring Study, northern Alaska, 2015.

every hour at 30 and 100 cm depths. Following deployment in September 2013, the Hobo Installations collected hourly soil temperature data throughout the winter and spring.

A field crew returned to service the Hobo Installations between 3 and 5 July 2014 following spring breakup of the Colville River. Each Hobo Installation was evaluated for damage and repaired or replaced if necessary. Any water observed in the boxes was drained (see Figure 14), each box was wiped dry, and the spent desiccant packet inside of the box was replaced. Any observations of damage, water penetrating the monitoring station box, or other disturbance were recorded and photos were taken of each station for documentation. Hobo Data Logger batteries were replaced and the data downloaded from each logger using a Hobo Waterproof Data Shuttle; the raw data files were backed up by downloading from the shuttle to a laptop in the field. The loggers were then re-deployed and left to collect hourly soil temperature data for another year.

The Hobo Installations were last visited between 6 and 9 August 2015 to download the data and remove installations from the 16 Permafrost Monitoring Plots. As in 2014, observations of damage, water penetration, or disturbance were recorded and photos were taken of each station for documentation. The GPS coordinates for all 16 Hobo Installations were evaluated to ensure

Figure 6. Snow survey field methods, CD5 Habitat Monitoring Study, northern Alaska, 2015. Field methods include a) accessing 16 Permafrost Monitoring Plots with in an all-terrain vehicle; b) recording snow depths along two, 25 m transects and at plot center; c) excavating small snow pits for snow density measurements; d) inserting the Snow-Hydro snow sampling tube into the profile to retrieve a snow core; e) extracting a snow core, ensuring all the snow is retained in the tube, and collecting only the snow in a sample bag; and f) recording snow sample weight and profile depth in a handheld computer.

Table 1. Cross-reference table between Hobo Installation superplot id, data logger serial number, subarea (Area ID), the date each Hobo Installation was installed and removed for 16 Permafrost Monitoring Plots, CD5 Habitat Monitoring Study, northern Alaska, 2013–2015.

Superplot ID	Hobo Serial No.	Area ID	Date Installed	Date Removed
rn-pc01	10392122	reference north	2013-09-10	2015-08-07
rn-pc02	10392123	reference north	2013-09-10	2015-08-07
rn-pc16	10392137	reference north	2013-09-13	2015-08-07
rs-pc09	10392130	reference south	2013-09-12	2015-08-09
rs-pc10	10392131	reference south	2013-09-12	2015-08-09
rs-pc11	10392132	reference south	2013-09-12	2015-08-09
tn-pc03	10392124	test north	2013-09-11	2015-08-08
tn-pc04	10392125	test north	2013-09-11	2015-08-08
tn-pc05	10392126	test north	2013-09-11	2015-08-06
tn-pc06	10392127	test north	2013-09-11	2015-08-09
tn-pc15	10392136	test north	2013-09-13	2015-08-09
ts-pc07	10392128	test south	2013-09-11	2015-08-06
ts-pc08	10392129	test south	2013-09-11	2015-08-08
ts-pc12	10392133	test south	2013-09-13	2015-08-08
ts-pc13	10392134	test south	2013-09-13	2015-08-08
ts-pc14	10392135	test south	2013-09-13	2014-07-05
ts-pc14	10392643	test south	2014-07-05	2015-08-09

accuracy of ±3 m relative to the actual position on the ground. Two Hobo Installation locations, tn-pc04 and rn-pc01, were inaccurate at greater than 3 m therefore the GPS coordinate were remeasured and the locations adjusted in the database to improve accuracy.

All fieldwork was based out of the Alpine Oil Facilities on the CRD. The Permafrost Monitoring Plots were accessed via helicopter in 2014, and by a combination of boat and truck in 2015.

OFFICE METHODS

DATA MANAGEMENT

DATA INTEGRATION

Climate and Snow Survey Data

Climate parameters recorded at the Alpine Weather Station are written to comma delimited (CSV) output files and transmitted via the AirLink Cellular Modem to Polar Alpine's host computer every hour. The files are then re-transmitted to ABR, Inc.—Environmental Research & Services (hereafter, ABR) where the data are inserted into the project database. Snow survey data for the snow depth measurements, density measurements, and general plot observations were imported into three tables in the project database (snow_data_depth, snow_data_swe, and snow_visit).

Soil Temperature Data

In the office, the raw Hobo data files were backed up on the ABR server. The raw files were converted to comma separated value (CSV) files and the timestamps, which were recorded on the Hobos in Alaska Daylight Savings time, were standardized to Coordinated Universal Time

Figure 7. Temperature Logger installation and field deployment, CD5 Habitat Monitoring Study, northern Alaska, 2013–2015. Installation includes a) feeding the HOBO logger cables through the water proof box and into the PVC tube to a depth of 11.8 in (30 cm) and 39.4 in (100 cm) from the soil surface; b) sealing the box and PVC tube and reinforcing connections with waterproof tape; c) removing and restoring the surface organic mat; and d) an image of the final logger installation.

(UTC) by adding 8 hours. The CSV files were then imported into the project database. All analyses were done using UTC times to avoid issues related to Daylight Saving Time transitions. Data from Hobo Installation tn-pc15 (Hobo serial number 10392136) were returned to the manufacturer, Onset Computer Corporation, for full data recovery. Data from paper field forms were entered by hand into digital format and the digital files were then proofed and uploaded to the project database.

DATA QUALITY CONTROL AND ASSURANCE

We ran several quality control and quality assurance (QAQC) routines on the climate and soil temperature data using both automated and hand filtering methods following Wells et al. (2015). The QAQC procedures were designed to ensure that only the highest quality data were used for analysis. No data were deleted from the database; instead, poor quality data records were flagged in the database and withheld from subsequent data analysis.

Snow survey data were entered directly into electronic forms and the majority of data entry QAQC was completed by carefully reviewing data each evening while in the field. In the office, the data were reviewed using basic data summaries to flag outliers.

DATA ANALYSIS

Data were analyzed using a combination of PostgreSQL (PostgreSQL Global Development Group 2015) queries, scripts written in R (R Development Core Team 2015), and data figures produced with the ggplot2 (Wickham 2009) R package. Database queries were formalized into views in the database, and all R code has been integrated into our revision control system.

CLIMATE DATA

Cumulative degree days were calculated as the sum of mean daily air temperatures (°C) at the Alpine Weather Station and Nuiqsut Airport National Weather Service Station where values were either above zero ("cumulative thawing degree days" [TDD]) or below zero ("cumulative freezing degree days" [FDD]). Thawing degree days are an index of warmth that relates to snowmelt, summer warmth, and the length of the growing season on the North Slope. Freezing degree days affect such processes as soil freezing and ice formation on waterbodies.

The weekly snow depth at the Alpine Weather Station was calculated from weekly median values. Climate data from three National Weather Service stations with long-term climate records, including Colville Village, Kuparuk, and Nuisqut Airport, were summarized to assess the climate during the monitoring period against climate normals. The maximum snow depths at the Alpine, Kuparuk, and Colville Village weather stations were estimated by aggregating snow depth data by week, and selecting the 80th percentile to reduce the variability associated with drifting and settling of fresh snowfall.

SNOW SURVEY DATA

Snow density was calculated for each snow core based the snow depth, snow weight, and cross-sectional area of the sampling tube:

$$\text{Snow Density (g/cm}^3\text{)} = \text{Snow Weight (g)} / (\text{Snow Depth [cm]} \times 30 \text{ cm}^2)$$

Snow water equivalent (SWE) for each core is equal to the snow depth times the density. To calculate the SWE for each snow-course following the double sampling method (Derry et al. 2009), the mean of the 50 snow-depth measurements was multiplied by the mean density of the 5 snow cores. The same calculation was performed to calculate the SWE for the cluster of snow-depth measurements surrounding each Permafrost Monitoring Plot waypoint.

The double sampling method was designed to be applied across the North Slope. Since the overall extent of the Permafrost Monitoring Plots is relatively compact (~3.5 km east–west and 7.3 km north–south) we also applied a snow density model (following Sturm et al. [2010]) that pooled all 80 of the snow cores to model snow density as a function of snow depth:

$$\text{Snow Density (g/cm}^3\text{)} = (\rho_{max} - \rho_0)\,[1 - \exp(-k \times \text{Snow Depth [cm]})\,] + \rho_0,$$

where ρ_0 is the initial snow density, ρ_{max} is the maximum snow density, and k is a fitting parameter. Starting values of ρ_0=0.2425, ρ_{max}=0.3630, and k=0.0029 were derived from Sturm et al. (2010) and the maximum likelihood method was used to fit the snow density model to the field data from the 80 snow cores. The snow density model was then used to estimate the density and SWE of each snow-depth measurement. The mean SWE for each plot by the snow density model method was calculated as the mean modeled SWE based on the 50 snow depths on the "L" transect at each plot.

Snow depth was summarized separately for the transect at each Permafrost Monitoring Plot, and for the cluster around the Hobo Installation at each plot. Snow depth summaries by transect, which reflect a broader area, were used to characterize the overall snow regime at each subarea. Snow depth summaries by cluster were prepared to understand the relationship between soil temperatures and snow depth at each plot because the cluster snow depths were tightly defined and better reflect the microclimate immediately around each Hobo Installation (particularly the shallower 30 cm temperature). Mean snow density was calculated for each Permafrost Monitoring Plot. SWE was then summarized for the transect at each Permafrost Monitoring Plot using both the double sampling method (Derry et al. 2009) and the snow density model.

SOIL TEMPERATURE DATA

Soil temperature data were analyzed by aggregating the soil temperature data to daily minimum, maximum, mean, standard deviation and median values for each depth and Hobo Installation for two time periods, including the "thaw season" (July 2014–September 2014) and the "freeze season" (October 2014–June 2015), to assess seasonal dynamics in soil temperature. These data were combined with hourly air temperatures received from the Alpine Weather Station, similarly aggregated to daily values so that all the temperature data could be examined together. The daily soil temperature data were also grouped by study area to compare the data at a broader spatial scale across the entire July 2014–June 2015 period.

Cumulative thawing and freezing n-factors were calculated as the ratio of seasonal degree day sums of the soil at 30 cm depth to the degree days of the air. N-factors are ideally calculated using air temperature measurements at 1–2 m above the ground surface, co-located with the soil temperature measurements (Klene et al. 2001, Karunaratne and Burns 2003). Site- specific air temperature was not measured in this study; instead, air temperature at weather stations located near the CD5 Monitoring Study Area were used to calculate n-factors. The CD5 Study Area is located approximately halfway between the Alpine Weather Station and the village of Nuiqsut; these locations span a latitudinal climate gradient, with higher TDDs to the south (see Climate Monitoring, below). The climate in the northern portion of the CD5 Study Area is more strongly influenced by the Beaufort Sea, leading to cooler summer temperatures than those found only a few miles farther inland. For instance, this is illustrated when comparing the long-term mean summer temperatures for the Colville Village (located at Helmericks' Homesite, Figure 1) and Nuiqsut Airport Weather Stations in Table 2. Hence, to better represent air temperatures in the CD5 Study Area, the mean between the Alpine Weather Station and Nuiqsut Airport mean daily air temperatures was used to calculate degree days of the air. One possible bias resulting from the use of a regional rather than site-specific air temperature to calculate n-factors is that thawing n-factors at plots to the south could be slightly overestimated, while those to the north could be slightly underestimated. The cumulative daily thawing and freezing n-factors were calculated for each Hobo Installation and then aggregated by subarea. N-factors should ideally be calculated using surface temperature (e.g., 1–5 cm deep); however, we followed the rationale of Karunaratne and Burns (2003) and used soil temperature at 30 cm with the assumption that soil temperatures measured at 30 cm provide a reasonable estimate of the near surface (≤5 cm deep) soil temperature. We acknowledge that temperatures at 30 cm will slightly overestimate surface temperature at the beginning of winter. Lastly, thawing n-factors were calculated for the period July 2014–September 2014, and freezing n-factors were calculated for the period October 2014–May 2015.

RESULTS AND DISCUSSION

CLIMATE MONITORING

AIR TEMPERATURE

Air temperatures over the study period ranged from -40.7 °C on 3 March 2015 to 25.9 °C on 20 June 2015 (Figure 8). The mean daily air temperature dropped below freezing in early October 2014, and remained below zero until mid-May 2015. The transitions between above and below freezing temperatures are closely linked with the onset of winter (and summer) and the development and loss of the snowpack shown in Figure 8.

We compared temperature data at the Alpine Weather Station between July 2014 and June 2015 with daily data from a similar period for the three closest active National Weather Service stations (NCEI 2015), and climate normal data for those stations (NCEI 2010) (Table 2). Mean air temperatures for summer 2014 (4.6 °C), winter 2014–2015 (-15.8 °C) and spring 2015 (8.8 °C) at

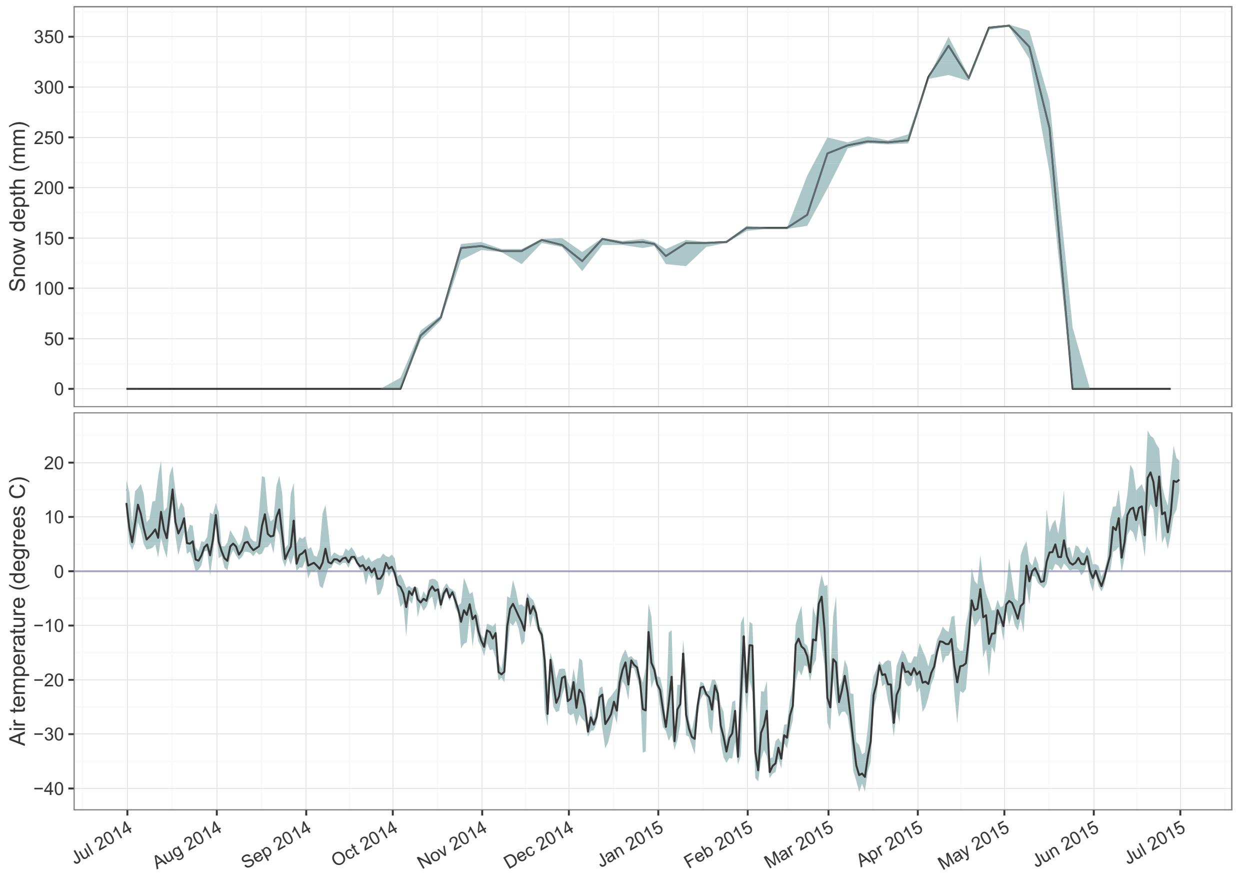

Figure 8. Median, 25th- and 75th-quartile of weekly snow depth, and average daily minimum, mean and maximum air temperature, at the Alpine Weather Station, Colville River Delta, northern Alaska, July 2014–June 2015.

the Alpine Weather Station were very similar to the temperatures reported by the National Weather Service stations. Stations reported slightly colder than normal summer 2014 temperatures, and warmer temperatures in winter 2014–2015 and spring 2015 (3.0 and 3.7 °C warmer than normal, respectively).

DEGREE DAYS

The progression of cumulative TDDs and FDDs at the Alpine weather station and the Nuiqsut Airport over the study period is presented in Figures 9 and 10. The pattern of cumulative FDDs is almost identical between the two stations, with rapid accumulation of FDDs between December and April. Alpine and Nuiqsut have a different pattern for TDDs, with warmer temperatures and higher TDD values throughout the spring and summer of 2014, as indicated by the higher absolute values and slope of the Nuiqsut cumulative thawing degree days chart.

PRECIPITATION

Precipitation is only measured during the summer months at the Alpine weather station, which makes it difficult to compare data from this station to nearby stations that collect precipitation data in winter by melting accumulated snow. Two of the three National Weather Service stations (Kuparuk and Colville Village) have both climate normal, and 2014–2015 precipitation data (Table 2). Precipitation was slightly below normal at these two stations in summer 2014, and above normal in winter 2014–2015. This matches the trend from the snow depth data for those two stations, which had higher than normal maximum snow depth during the winter (see below).

Table 2. Comparison of 2014–2015 seasonal averages for air temperature, precipitation, and snow depth to 30-year normals for Alpine, Colville Village, Kuparuk and Nuiqsut Airport, CD5 Habitat Monitoring Study, northern Alaska, July 2014–June 2015.

Weather Station	Season[1]	Normal Mean Temp[2] (°C)	Mean Temp (°C)	Mean Temp Anomaly (°C)	Normal Precip.[2] (mm)	Total Precip. (mm)	Total Precip. Anomaly (mm)	Normal Snow Depth[2] (mm)	Max. Snow Depth (mm)	Snow Depth Anomaly (mm)
Alpine	Summer 2014	NA	4.6	NA	NA	not shown[3]	NA	NA	0	NA
Alpine	Winter 2014-2015	NA	-15.8	NA	NA	not shown[3]	NA	NA	359	NA
Alpine	Spring 2015	NA	8.8	NA	NA	not shown[3]	NA	NA	0	NA
Colville Village	Summer 2014	4.7	4.2	-0.5	72	66	-6	12	0	-12
Colville Village	Winter 2014-2015	-19	-15.8	3.2	46	66	20	277	305	28
Colville Village	Spring 2015	3.6	7.6	4	6	20	14	52	0	-52
Kuparuk	Summer 2014	6.2	4.8	-1.4	60	52	-8	15	0	-15
Kuparuk	Winter 2014-2015	-18.7	-15.8	2.9	29	97	68	291	432	141
Kuparuk	Spring 2015	5.2	8.8	3.6	8	5	-3	10	0	-10
Nuiqsut Airport	Summer 2014	6.4	5.6	-0.8	NA	NA	NA	NA	NA	NA
Nuiqsut Airport	Winter 2014-2015	-18.7	-15.9	2.8	NA	NA	NA	NA	NA	NA
Nuiqsut Airport	Spring 2015	6.2	9.7	3.5	NA	NA	NA	NA	NA	NA

1 Seasons are defined as summer(July–September), winter (October–April), and spring (May–June).
2 Normals refer to averaged, smoothed data from longest available period-of-record for each station from 1981 to 2010.
3 Summer precipitation data at the Alpine weather station is measured differently than at other stations reported here, hence data are not shown.

WIND

Winds at the Alpine weather station are rarely calm, varying in direction and speed by season (Figure 11). The strongest winds were in early (October and November 2014) and late winter (April 2015), when winds primarily came from the east and northeast. Wind direction is more variable during other months, but primarily is still easterly to northeasterly except during January–March, when it is often blowing from west to southwest.

SNOW DEPTH

Snow depth at Alpine, paired with air temperature (Figure 8), shows snow accumulation began almost immediately after the temperature dropped below zero in early October, and

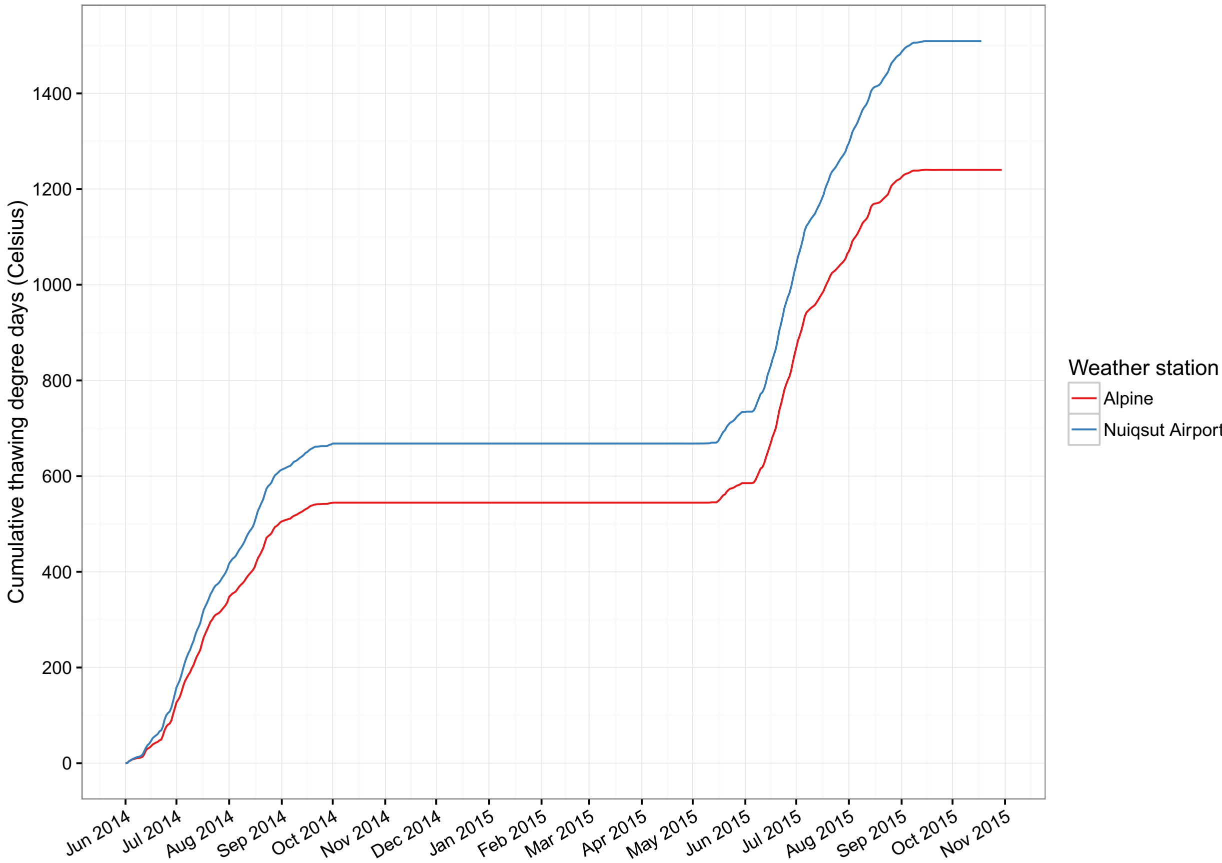

Figure 9. Cumulative thawing degree days (TDD) for the Alpine Weather Station and the Nuiqsut Airport National Weather Service Station, June 2014–September 2015.

continued until the third week in October. Other periods of accumulation occurred at the end of February 2015 and in early April. The snow at Alpine melted rapidly beginning in the first week of May and was gone by June. Weekly snow-depth summaries from the first week of September 2014 through the end of June 2015 are presented in Appendix A-1.

Snow depth at the Alpine weather station during the snow survey (7–9 April 2015; see next section) was fairly stable, ranging from 306 to 312 mm with a mean depth of 310 mm (Appendix A-1). The maximum estimated depth at the Alpine weather station (359 mm) was intermediate between the values for the nearby Colville Village (305 mm) and Kuparuk Airport (432 mm) stations in late April 2015 (Table 2). Both the Colville Village and Kuparuk Airport stations had above-normal maximum snow depth for winter 2014–2015. The Kuparuk Airport station, however, was almost 50% higher than normal while Colville Village was only 10% higher. The variability between stations for snow depth makes it difficult to make strong conclusions about how the winter 2014–2015 snowpack in the CD5 Habitat Monitoring Study Area compares with a normal winter, but it was presumably at least somewhat deeper than normal.

SNOW SURVEYS

Snow surveys were conducted 7–9 April 2015. The mean daily air temperatures were -17.2, -14.0, and -13.3°C on 7, 8, and 9 April, respectively. Winds were from the northeast and were very strong on 7 and 8 April (mean daily wind speeds of 12.2 and 8.5 m/s, respectively).The mean wind speed slowed to 2.7 m/s on 9 April 2015. Active drifting of surface snow occurred during field surveys on the first two days, and about 10 mm of new fresh snow was present above

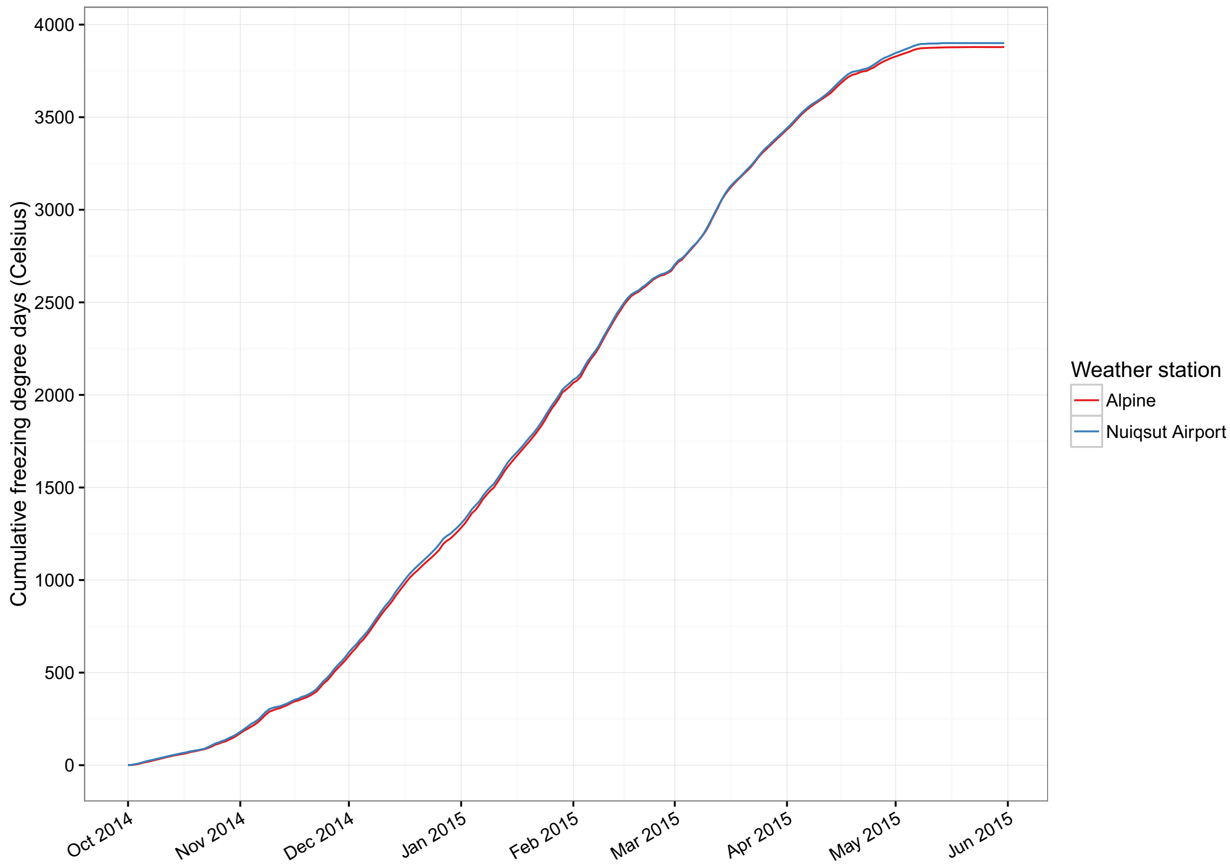

Figure 10. Cumulative freezing degree days (FDD) for the Alpine Weather Station and the Nuiqsut Airport National Weather Service Station, October 2014–May 2015.

the wind-hardened snowpack on 9 April. No evidence of melting was observed at any of the plots and mean temperatures at the snow–ground interface measured while collecting snow cores ranged from -12.1 to -15.9 °C. These basal temperatures increased each day during the survey in response to the increasing air temperatures. Vegetation was almost entirely overtopped by snow at all the plots, with only a few protruding shrubs and graminoid stems. An ice layer approximately 10 mm thick was observed in the snowpack in many snow cores, and the presence/absence of ice layer(s) was recorded systematically starting on 8 April 2015. An ice layer was present in 65% of cores at depths (measure below the snow surface) ranging from 50–230 mm. The ice layer was probably associated with a rain-on-snow event that most likely occurred in late February 2015 (Figure 8).

At the time of sampling, there was no evidence of disturbance at any of the Permafrost Monitoring Plots. None of the Hobo Installations were exposed and none of them were detected by manually probing the snowpack during the field surveys.

Snow depths were measured systematically on 50 m long “L” transects in the vicinity of each Hobo location to characterize the local area, and also in a cluster of ≥10 points immediately surrounding the Hobo Installation to characterize the microsite in which the Hobo was installed. Individual snow depths ranged 60–635 mm. Mean snow depths for the “L” transects ranged 205–347 mm, with an overall mean snow depth of 279 mm across all transects. This was 31 mm less than the 310 mm mean snow depth observed at the Alpine weather station during 7–9 April 2015.

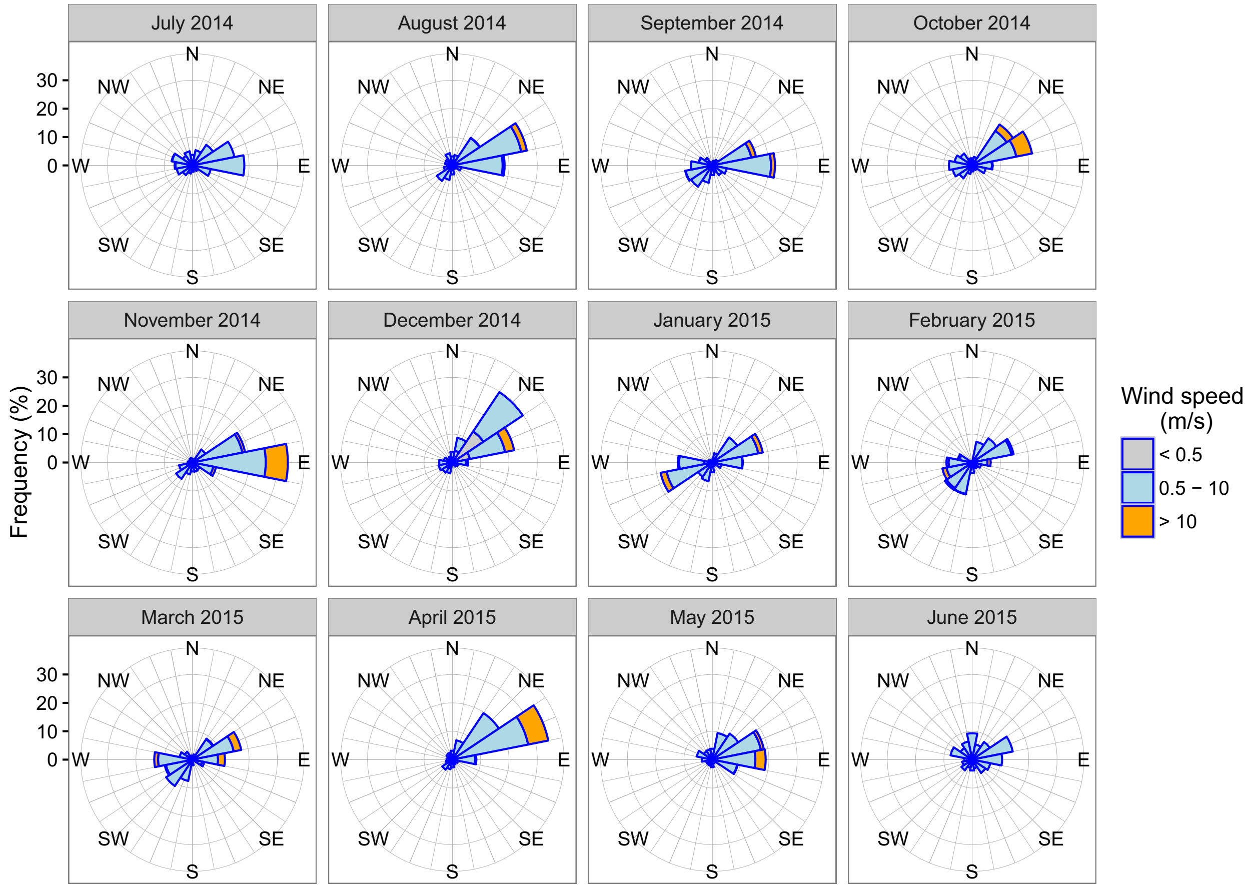

Figure 11. Charts summarizing monthly wind speed and direction at the Alpine Weather Station, Colville River Delta, northern Alaska, July 2014–June 2015.

The mean snow depth at Hobo locations ranged from 158 to 396 mm, with a mean of 277 mm (Table 3). Seven plots had deeper snow at the plot center, whereas nine had deeper snow on the "L" transect (Table 3). At two plots the difference was ≥90 mm. The bias between snow depths measured at Hobo locations and transects was very small, however, with a mean difference of only 2 mm. The mean absolute difference of snow depths at Hobo locations compared to "L" transects was 37 mm.

Based on the snow depths measured at transects, plots can be grouped into three depth classes: ≤248 mm snow depth (four shallow plots); 269–290 mm snow depth (eight intermediate plots); and ≥322 mm snow depth (four deep plots) (Table 3). Vegetation class appears to be an important factor influencing snow depth: all of the shallow snow plots had Wet Sedge Meadow Tundra vegetation, whereas 75% of the deep snow plots had Wet Sedge-Willow Tundra vegetation. The eight intermediate-depth plots were split evenly between graminoid-dominated vegetation and shrub-dominated vegetation. Shrub abundance appears to play a key role in trapping snow in the study area, as even sparse, low-statured shrub vegetation tends to have higher snow-holding capacity than graminoid-dominated tundra (Sturm et al. 2001). There was no clear relationship between snow depth and surface form at the plots (Table 3), though all of the shallow snow plots were in the centers of low-relief, low-centered polygons.

Mean snow density, based on the five snow cores at each plot, ranged from 0.25 to 0.32 g/cm³ (Table 3). No clear relationship between snow density and other plot parameters was apparent. The presence and thickness of wind slab and ice layers would be expected to increase snow density, but data were not collected systematically on these parameters (except for presence/absence and depth of an ice layer on the latter two days of the survey). Point-measurements of snow density can vary due to sampling error and snowpack variation (including voids caused by vegetation), and this presumably accounts for some of the variability between plots.

Snow depth can be one of the most important factors explaining variation in snow density hence, snow density was modeled as a function of snow depth (Figure 12). The fitted model with snow depth as the predictor explained >30% of the variance in snow density with parameters of ρ_0=0.1632, ρ_{max}=0.3504, and k=0.0340. The modeled density increased with snow depth from ~0.17 g/cm³ for the shallowest snow, to ~0.33 g/cm³ for the deepest observed snow.

SWE for each plot was calculated using the double sampling method (Derry et al. 2009) and the snow density model (Table 3). Overall, SWE was similar with the two methods with the largest difference at plot ts-pc07 (68.4 mm by the double sampling method and 57.6 mm using the snow density model). Plot ts-pc07 had the second lowest snow depth and the highest mean density; the two highest snow densities were measured at cores on that plot, which were measured over ice rather than tundra vegetation. Only 9% of cores we sampled were over ice. For all the plots, SWE calculated by the two methods was similar, with the density model method averaging 1.5 mm higher SWE. The mean absolute difference between the two SWE estimation methods was 4.4 mm.

We consider the snow density model approach to be more robust because the study area is fairly compact and is unlikely to have different snow regimes, and because the relationship between snow depth and snow density is well established (Sturm 2010). This relationship was also borne out by our field data. When SWE is estimated based on the density model, SWE ranges from 53.7 to 102.0 mm. The plots group into the same shallow (≤67.6 mm SWE), intermediate (75.1–81.6 mm SWE), and deep (≥93.4 mm SWE) categories, with graminoid-dominated tundra holding less snow than shrubby tundra.

We recorded the thickness of the depth hoar layer at each core, since depth hoar is a highly insulative type of snow (Sturm et al. 2001). Mean depth hoar by plot ranged from 94 to 194 mm with a mean thickness of 142 mm. Excluding the minimum and maximum values, the range of depth hoar thicknesses was 114–160 mm. No clear trends were apparent relating depth hoar to snow depth or site properties. Depth hoar thickness has been used in combination with wind slab thickness to estimate the bulk thermal resistance of the snowpack (Sturm et al. 2001).

When the data were aggregated to subarea (Table 4, Figure 13), snow was deepest in the Test Area North subarea (298 mm) and shallowest in the Test Area South subarea (252 mm). Reference Area North and Reference Area South had snow depths of 284 and 286 mm, respectively. The pattern is largely driven by the spatial distribution of the snow depth groupings: the Test Area North subarea has two of the four deep snow (shrubby) plots, the Test Area South subarea had two of the four shallow snow (graminoid-dominated) plots, and the two reference areas each had one deep snow plot and one shallow snow plot. Density measurements were similar in all subareas, ranging from 0.27 to 0.28 g/cm³. SWE by the density model method ranged from 69.4 to 85.1 mm, with Test Area North having the highest SWE and Test Area South having the lowest SWE. Thickness of depth hoar ranged from 139 to 148 mm and was thicker in the Reference Area North and Test Area North subareas.

SOIL TEMPERATURE MONITORING

FIELD OBSERVATIONS

Spring breakup on the Colville River in 2015 was a high magnitude, short duration event (Baker 2015) that flooded the majority of the CD5 Habitat Monitoring Study Area (Figure 2). Observations made during the 6–9 August 2015 fieldwork indicated that 15 of the 16 Hobo Installations were flooded during spring breakup. Permafrost Monitoring Plot tn-pc04 was the only location that lacked evidence of 2015 spring breakup flooding (e.g., woody debris, silt coats on vegetation, etc.). Aerial images, taken on 22 May 2015 at 1143 local time by Michael Baker Jr., Inc. (Baker), suggest that tn-pc04 was either outside of the flood zone, or

Table 3. Summary of snow survey and selected environmental data by Permafrost Monitoring Plot (PMP), including snow depth, snow density, snow water equivalent (SWE), depth hoar thickness, temperature at base of snow pack, surface form, and Alaska Vegetation Classification (AVC) Level 4 vegetation class, CD5 Habitat Monitoring Study, northern Alaska, April 2015.

Superplot ID	Survey Date	Hobo Mean Snow Depth (mm)	Std. Dev. Hobo Snow Depth (mm)	"L" Transect Mean Snow Depth (mm)	Std. Dev. "L" Transect Snow Depth (mm)	Mean Density of Snow Cores at PMP (g/cm^3)	SWE, Double Sampling Method (mm)[1]	SWE, Density Model Method (mm)	Mean Thickness Depth Hoar (mm)	Mean Temp at Base of Snow (°C)	Number of Snow Depths at Hobo	Number of Snow Depths at "L" Transect	Surface Form	AVC Level 4 Veg Class
rn-pc01	2015-04-08	259	31	280	53	0.28	78.2	78.3	134	-12.7	10	50	Low-centered, Low-relief, Low-density Polygons	Wet Sedge Meadow Tundra
rn-pc02	2015-04-08	158	29	248	71	0.26	63.9	67.6	150	-13.4	11	52	Low-centered, Low-relief, Low-density Polygons	Wet Sedge Meadow Tundra
rn-pc16	2015-04-08	331	25	323	65	0.26	84.4	93.6	154	-12.3	10	50	Low-centered, Low-relief, High-density Polygons	Wet Sedge Meadow Tundra
rs-pc09	2015-04-09	235	39	238	57	0.25	59.4	64.1	136	-12.8	12	51	Low-centered, Low-relief, High-density Polygons	Wet Sedge Meadow Tundra
rs-pc10	2015-04-09	396	39	347	76	0.28	98.7	102.0	158	-12.7	12	50	Low-centered, Low-relief, Low-density Polygons	Wet Sedge-Willow Tundra
rs-pc11	2015-04-09	248	59	274	76	0.27	74.4	76.5	124	-12.1	22	50	Low-centered, High-relief, High-density Polygons	Wet Sedge Meadow Tundra
tn-pc03	2015-04-08	273	38	331	72	0.31	102.4	96.4	154	-12.4	12	51	Low-centered, Low-relief, Low-density Polygons	Wet Sedge-Willow Tundra
tn-pc04	2015-04-08	262	26	286	81	0.27	78.1	80.7	156	-13.0	11	51	Low-centered, Low-relief, Low-density Polygons	Wet Sedge-Willow Tundra
tn-pc05	2015-04-08	262	88	283	77	0.25	69.6	79.7	160	-13.2	10	50	Low-centered, Low-relief, High-density Polygons	Wet Sedge Meadow Tundra
tn-pc06	2015-04-08	299	101	322	92	0.29	94.2	93.4	114	-14.0	10	50	Low-centered, High-relief, High-density Polygons	Wet Sedge-Willow Tundra
tn-pc15	2015-04-07	222	37	269	90	0.30	80.5	75.1	156	-15.9	11	50	Low-centered, Low-relief, Low-density Polygons	Wet Sedge-Willow Tundra
ts-pc07	2015-04-08	310	87	217	77	0.32	68.4	57.6	94	-14.7	10	50	Low-centered, Low-relief, High-density Polygons	Wet Sedge Meadow Tundra
ts-pc08	2015-04-07	324	101	270	99	0.27	73.9	75.9	118	-14.1	10	50	Polygon Rims	Moist Sedge-Shrub Tundra
ts-pc12	2015-04-07	309	75	279	68	0.25	68.5	78.3	152	-14.1	10	50	Low-centered, Low-relief, Low-density Polygons	Wet Sedge Meadow Tundra
ts-pc13	2015-04-07	330	45	290	58	0.28	81.3	81.6	194	-13.5	10	50	Low-centered, Low-relief, Low-density Polygons	Wet Sedge-Willow Tundra
ts-pc14	2015-04-07	213	64	205	74	0.26	53.8	53.7	116	-14.1	10	50	Low-centered, Low-relief, Low-density Polygons	Wet Sedge Meadow Tundra
Mean of All Plots		277	55	279	74	0.28	76.9	78.4	142	-13.4				

[1]Derry et. al 2009

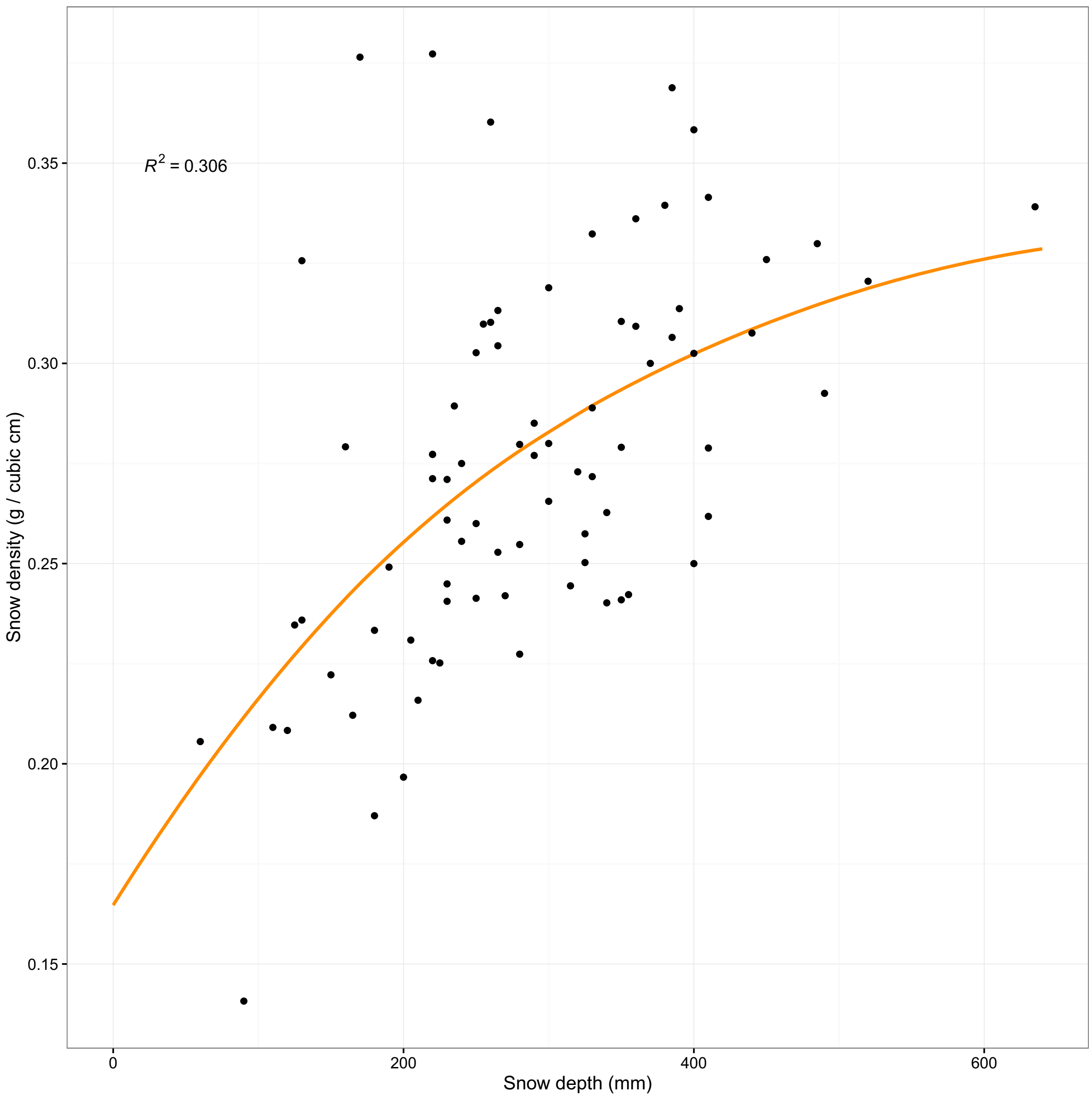

Figure 12. Snow density as a function of snow depth, CD5 Habitat Monitoring Study, northern Alaska, April 2015.

Table 4. Snow survey data from Permafrost Monitoring Plots (PMP) aggregated by subarea, including snow density, snow water equivalent (SWE), depth hoar thickness, temperature at base of snow pack, and average snow depth, CD5 Habitat Monitoring Study, northern Alaska, April 2015.

Area ID	Count of PMP	"L" Transect Mean Snow Depth (mm)	Mean Density of Snow Cores in Subarea (g/cm^3)	Mean SWE, Double Sampling Method (mm)[1]	Mean SWE, Density Model Method (mm)	Mean Thickness Depth Hoar (mm)	Mean Temp at Base of Snow (°C)
reference north	3	284	0.27	75.5	79.8	146	-12.82
reference south	3	286	0.27	77.5	80.9	139	-12.53
test north	5	298	0.28	85.0	85.1	148	-13.70
test south	5	252	0.28	69.2	69.4	135	-14.09

[1] Derry et. al 2009

only briefly inundated during peak discharge (pers. comm. Yager). All 16 Permafrost Monitoring Plots had evidence of water inside the waterproof PVC box (Figure 14). The amount of water in Hobo Installation boxes, ranged from 1 cm to several centimeters and presumably resulted in 3 Hobo Data Loggers (rs-pc11, ts-pc14, and tn-pc15) being inoperable at the time of the August 2015 field visit. We believe that instances where several centimeters of water penetrated the boxes are related to both failure of the rubber stopper seals placed at the bottom of the PVC tube that houses the Hobo Logger sensors, and from the exceptional spring breakup flooding conditions in May 2015. Given that nearly all Hobo Installations were installed in wet sedge meadows in low-centered polygons—in some cases in several centimeters of standing water—it is not too surprising that water was found inside all the boxes.

Baker (2015) reported large areas of the CD5 Study Area were inundated during 2015 spring breakup. Flooding resulted in disturbance or damage to several of the Hobo Installations. For instance, 5 Hobo Installations adjacent to the Niġliq Channel were either lightly damaged, flipped upside down, and/or disconnected at the L-joint (Figures 2 and 14). Damage to the L-joint led to excess Hobo Logger cable, that was stored inside the PVC box, to be exposed above ground (Figure 14). Additionally, two Hobo Installations in Test Area South, upstream of the CD5 road, were also damaged at breakup (Figure 2).

DATA SUMMARIES BY PERMAFROST MONITORING PLOT

General Trends

Appendix B presents time-series of median daily soil temperature at each Permafrost Monitoring Plot and the mean daily air temperature at the Alpine Weather Station from the beginning of July 2014 through the end of June 2015. The 16 charts show that while the absolute soil temperatures differed to varying degrees between each Hobo Installation, the overall temperature dynamics were similar over the study period.

In general, soil temperature patterns during the monitoring period followed the mean air temperature, with a lag time in the response of soil temperatures depending on depth. Time-series of median daily temperature for each plot showed some common trends across all Permafrost Monitoring Plots (Appendix B). On July 1, all soil temperatures at 30 cm were at or above 0 °C and remained so through mid- to late-September. Soil temperatures at 30 cm fluctuated up and down several degrees from July through mid-August, corresponding to the general air temperature pattern; the corresponding changes in soil temperature at 30 cm lagging slightly behind

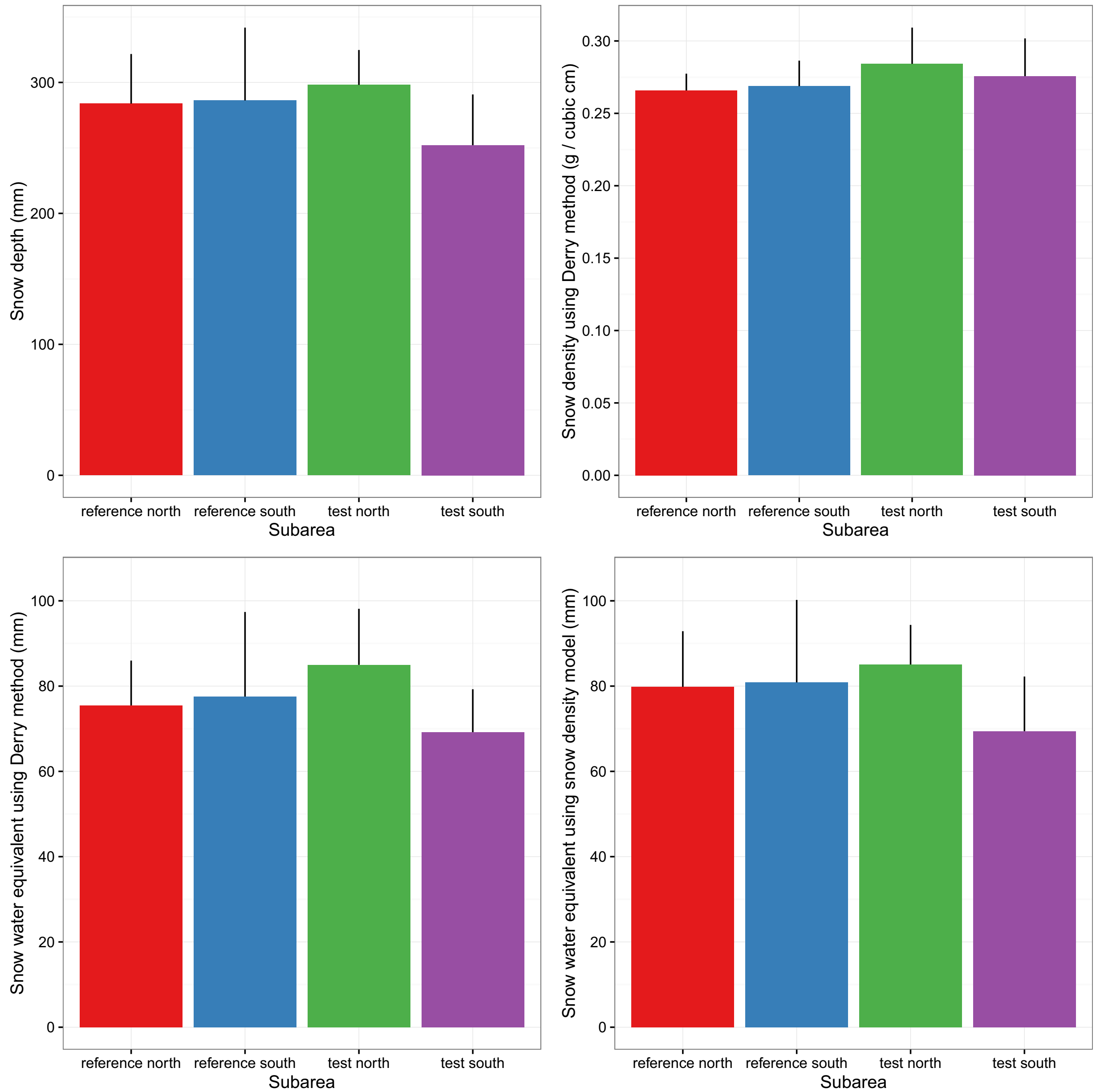

Figure 13. Bar charts summarizing snow characteristics by subarea, including average and standard deviation of snow depth, snow density, snow water equivalent (SWE) calcuated using the Derry et al. 2009 method, and SWE calculated using the snow density model, CD5 Habitat Monitoring Study, northern Alaska, 2015.

Figure 14. Photos of water in the bottom of a Hobo Installation box at RN-PC01 (top) and t-joint disconnected at plot TS-PC08 (bottom) resulting from disturbance by spring breakup flooding, CD5 Habitat Monitoring Study, northern Alaska, 2015.

change in air temperature and with less variability (i.e., lower amplitude and frequency of oscillations). In mid- to late-August, the soil temperature at 30 cm begins a slow, steady decline through late September, again following the general trend in air temperature. The soil temperature at 100 cm from July through late September showed a very gradual warming, with temperature reaching approximately -1 °C. By early September, the 100 cm soil temperature reached a maximum at which point the temperature flatlined for several months. The 30 cm temperatures dropped to 0 °C by mid- to late-September and held there for nearly 3 months, despite fluctuations in air temperature between 0 °C and -18 °C. This period is referred to as the zero curtain effect and represents the period when all heat flux is dedicated to the phase change of soil water from liquid to solid (i.e., latent heat of fusion) rather than sensible heat. This effect is a common characteristic of wet, medium-texture mineral and organic soils during freezing (Outcalt et al. 1990). In mid-December, the 30 cm temperatures abruptly dropped which represents the point where all of the liquid soil water is frozen and soil temperature again becomes responsive to air temperature. During this time the 100 cm temperature lagged behind the 30 cm for several days to a few weeks but eventually also dropped. During this time, the 30 cm temperatures dropped below the 100 cm temperatures, a trend that continued through mid-April. The cooling trend continued until the first trough for both 30 and 100 cm temperatures in late January, corresponding to a drop in air temperature to approximately -30 °C. This drop in temperature was followed by a peak in early February corresponding to about a week of temperatures above -20 °C, and then a second trough in mid-February corresponding to a drop in air temperature to nearly -35 °C. In early March, a second peak in soil temperature at both 30 cm and 100 cm occurred that was associated with a rise in air temperature above -10 °C. During this period, the 30 cm soil temperature warms up to nearly the temperature at 100 cm. This warming period is followed by a drop in soil and air temperatures in mid-March, evident as another trough in the time-series. Following this mid-March cold period, the trend in soil temperature at both 30 and 100 cm is generally upward for the remainder of winter and into the spring and summer. Again, the soil temperatures follow the general trend in air temperature, but with a time lag and a lower magnitude and frequency of diurnal oscillations. The 30 cm soil temperature began to exceed the 100 cm soil temperature by mid- to late-April. By mid-May, the soil temperature at both depths reached inflection points at approximately the same time that the air temperatures began rising above 0 °C. From mid-May through June, the soil temperature began to climb slowly; the 30 cm soil temperature rising above 0 °C in mid- to late-June. In late May several Hobo Installations recorded a short, sharp spike (i.e., 1–2 °C change in <24 hours) in temperature at 30 cm (e.g., Appendix B-14). This spike in temperature at 30 cm may be related to a warming of the soil active layer due to the loss of snow cover and heat advection by spring breakup floodwaters. Breakup flooding peaked along the Niġliq Channel and all CD5 Road bridge crossings on 22 May 2015 (Baker 2015), within a few hours to several days of the spike in 30 cm soil temperature at several Hobo Installations. Breakup floodwaters, while near freezing in temperature, were much warmer than soil temperature; this could have caused a temporary warming effect in the upper portion of the soil profile if inundation lasted for more than a few hours. The spike in soil temperature was not recorded at any of the Hobo Installations at the 100 cm depth, which were strongly buffered from rapid changes in surface conditions.

The exception to the general pattern in soil temperatures described is the 30 cm soil temperature at plot tn-pc15. While the temperature at 30 cm at all other plots dropped to 0 °C in late September and remained there for several months, the 30 cm temperature at plot tn-pc15 dropped below 0 °C in late September (Appendix B-11). The 30 cm temperature dropped below the 100 cm soil temperature soon thereafter and held around -2°C for several months until mid-December, after which the 30 cm temperature trend followed a similar pattern observed at the other 15 plots. Plot tn-pc15 was also the last plot to see the 30 cm soil temperatures rise above the 100 cm temperature in early-May while soil temperature at 30 cm at all other plots surpassed 100 cm temperatures in mid- to late-April. For the remainder of the monitoring period the 30 cm temperature trend at plot tn-pc15 followed a similar pattern observed at the other 15 plots. The 100 cm soil temperature at plot tn-pc15 followed a similar pattern as other plots throughout the monitoring period. Plot tn-pc15 also had the coldest mean annual soil temperature at 30 cm (Table 5). The soil temperature trend at plot tn-pc15 observed during the current monitoring year were not observed in the previous year (Wells et al. 2014), and the Hobo Installation at plot tn-pc15 was not located under an ice pad or road (pers. comm. Davis-Turak). The similar 30 cm temperature trends from December through March, and May through June, in addition to the similarity between the 100 cm soil temperatures throughout the monitoring period, suggest that the Hobo unit was not obviously impaired during these periods. However, the Hobo datalogger at this plot was not operational in August 2015 and this datalogger was returned to the manufacturer for data recovery. A review of the temperature data on this logger indicates that the logger continued to collect data through early July 2015 after which the data logger failed. This suggests that the soil temperature data observed at plot tn-pc15 is suspect. The lack of a zero curtain at this plot in early winter indicates that the data logger may have begun failing as early as September 2014. As such, soil temperature data from this logger were withheld from the soil data summaries by subarea (see Data Summaries by Reference and Test Areas, below).

Seasonal Summaries by Plot

Summary statistics (July 2014–September 2014) of cumulative thickness of organic soil materials; maximum active layer depth; and daily minimum, maximum, mean, standard deviation and median values of soil temperature are presented in Table 5. The 30 cm sensor at all Hobo Installations was positioned within the active layer (seasonally frozen soil), which is evident in the time-series in Appendix B, where the 30 cm temperatures are usually above 0°C in July, August, and most of September. The mean temperature at 30 cm during the thaw season ranged between 0.70 °C (± 0.56 °C) and 2.76 °C (± 1.38 °C). The coldest mean temperatures during the thaw season at 30 cm were observed at plot ts-pc13 and the warmest at rs-pc10. The mean temperatures at 100 cm during the thaw season were slightly colder than those at 30 cm, ranging from -1.31 °C (± 0.40 °C) to -0.98 °C (± 0.30 °C). The coldest mean temperature during the thaw season at 100 cm was observed at ts-pc07, and the warmest at plot ts-pc12.

Table 6 shows summary statistics including daily minimum, maximum, mean, standard deviation and median values for each depth; cumulative thickness of organic soil materials; and active layer depth at the 16 Permafrost Monitoring Plots for the freeze season, October 2014–June 2015. The mean temperature at 30 cm during the freeze season ranged between -7.39 °C (± 6.06 °C) and -5.61 °C (± 5.69 °C). The coldest mean temperatures during the freezing period at 30 cm were observed at plot tn-pc15 and the warmest at rs-pc10. The mean temperatures at 100 cm during the freeze season were slightly colder than those at 30 cm ranging from -6.86 °C (± 5.05 °C) to -5.21 °C (± 4.29 °C). The coldest mean temperature at 100 cm during the freeze season was at plot rn-pc02, and the warmest was observed at rs-pc10; the same plot with the warmest mean temperature at 30 cm.

Soil Temperature and Environmental Factors

The absolute temperature differences observed between the individual Permafrost Monitoring Plots may in part be related to differences in site-specific air temperatures. The Alpine Weather Station is located approximately 7–12 km to the northeast of the Permafrost Temperature Monitoring Plots. While these station data are broadly representative of the western CRD, it may not represent the site-specific air temperature at each Hobo Installation. Air temperature is not available for each Hobo Installation, therefore our comparisons are limited to the air temperature of the general area. In general, we observed that soil temperature was quite responsive to changes in air temperature. The 30 cm temperatures tended to respond more quickly and to a greater magnitude than the 100 cm temperatures, rising several degrees above 0 °C in the summer months and dropping into the negative teens in the winter months. In addition, whereas the mean air temperatures can fluctuate rapidly up or down, sometimes on a daily basis, the soil temperatures were more stable and typically trended in a given direction (flat line, up, or down) for several days to weeks before changing

Table 5. Soil temperature summary statistics at 30 cm and 100 cm, cumulative organic thickness (cm) within the active layer, active layer depth (cm), and cumulative thawing n-factor for individual Hobo Installations at 16 Permafrost Monitoring Plots, CD5 Habitat Monitoring Study, northern Alaska, July 2014–September 2014.

Superplot ID	Area ID	Cum. Org. Thickness in Active Layer (cm)	Active Layer Depth (cm)	Min. Temp at 30 cm (°C)	Mean Temp at 30 cm (°C)	Std. Dev. Temp at 30 cm (°C)	Median Temp at 30 cm (°C)	Max. Temp at 30 cm (°C)	Temp Obs. at 30 cm	Min. Temp at 100 cm (°C)	Mean Temp at " 100 cm (°C)	Std. Dev. Temp at 100 cm (°C)	Median Temp at 100 cm (°C)	Max. Temp at 100 cm (°C)	Temp Obs. at 100 cm	Cum. Thawing n-factor
rn-pc01	reference north	48.0	51.0	-0.37	1.29	0.85	1.32	3.51	2208	-1.87	-1.00	0.36	-0.90	-0.62	2208	30
rn-pc02	reference north	49.0	50.0	0.02	1.59	0.80	1.70	3.49	2208	-2.07	-1.18	0.37	-1.07	-0.76	2208	35
rn-pc16	reference north	48.0	50.0	-0.03	1.84	0.99	1.94	4.43	2201	-2.04	-1.21	0.37	-1.10	-0.79	2207	41
rs-pc09	reference south	49.5	55.0	0.05	2.42	1.16	2.69	4.77	2207	-1.93	-1.11	0.36	-1.02	-0.70	2207	51
rs-pc10	reference south	48.0	55.0	-0.09	2.76	1.38	3.14	5.15	2208	-1.93	-1.10	0.34	-1.02	-0.70	2205	57
rs-pc11	reference south	42.0	49.0	-0.06	1.96	0.99	2.13	4.09	2207	-1.81	-1.03	0.33	-0.93	-0.65	2207	41
tn-pc03	test north	35.0	37.0	0.00	2.05	0.94	2.29	3.88	2207	-1.87	-1.13	0.32	-1.04	-0.79	2205	44
tn-pc04	test north	43.0	46.0	-0.20	1.10	0.68	1.15	2.77	2207	-1.93	-1.10	0.34	-1.02	-0.73	2204	26
tn-pc05	test north	32.0	36.0	-0.12	1.61	0.92	1.75	3.78	2208	-2.04	-1.16	0.39	-1.04	-0.73	2208	35
tn-pc06	test north	37.0	37.0	-0.14	1.17	0.78	1.15	3.33	2207	-2.10	-1.30	0.35	-1.21	-0.90	2207	27
tn-pc15	test north	48.0	51.0	-0.99	1.56	1.24	2.02	3.67	2207	-1.76	-1.07	0.30	-0.96	-0.73	2203	29
ts-pc07	test south	24.0	42.0	-0.12	1.62	0.89	1.75	3.70	2207	-2.22	-1.31	0.40	-1.19	-0.85	2207	35
ts-pc08	test south	15.0	46.0	0.00	1.83	1.16	1.83	4.97	2207	-1.96	-1.01	0.40	-0.90	-0.56	2207	42
ts-pc12	test south	50.0	52.0	0.02	2.50	1.21	2.77	5.08	2172	-1.67	-0.98	0.30	-0.90	-0.65	2207	53
ts-pc13	test south	43.0	44.0	-0.37	0.70	0.56	0.69	2.13	2208	-1.99	-1.26	0.32	-1.19	-0.90	2208	18
ts-pc14	test south	46.0	51.0	0.02	1.65	0.83	1.72	3.70	2183	-1.99	-1.12	0.35	-1.02	-0.73	2183	35

Table 6. Soil temperature summary statistics at 30 cm and 100 cm, cumulative organic thickness (cm) within the active layer, active layer depth (cm), and cumulative freezing n-factor for individual Hobo Installations at 16 Permafrost Monitoring Plots, CD5 Habitat Monitoring Study, northern Alaska, October 2014–June 2015.

Superplot ID	Area ID	Cum. Org. Thickness in Active Layer (cm)	Active Layer Depth (cm)	Min. Temp at 30 cm (°C)	Mean Temp at 30 cm (°C)	Std. Dev. Temp at 30 cm (°C)	Median Temp at 30 cm (°C)	Max. Temp at 30 cm (°C)	Temp Obs. at 30 cm	Min. Temp at 100 cm (°C)	Mean Temp at 100 cm (°C)	Std. Dev. Temp at 100 cm (°C)	Median Temp at 100 cm (°C)	Max. Temp at 100 cm (°C)	Temp Obs. at 100 cm	Cum. Freezing n-factor
rn-pc01	reference north	48.0	51.0	-16.70	-6.33	6.10	-4.50	3.88	6550	-13.35	-5.90	4.81	-4.74	-0.59	6552	119
rn-pc02	reference north	49.0	50.0	-16.83	-7.17	6.45	-7.67	2.58	6550	-13.89	-6.86	5.05	-6.58	-0.73	6552	135
rn-pc16	reference north	48.0	50.0	-15.31	-6.05	5.81	-3.90	2.26	6533	-12.23	-5.78	4.53	-4.80	-0.73	6552	121
rs-pc09	reference south	49.5	55.0	-18.97	-6.78	6.68	-5.62	3.62	6548	-14.71	-6.41	5.15	-5.30	-0.62	6552	123
rs-pc10	reference south	48.0	55.0	-15.71	-5.61	5.69	-2.33	3.78	6472	-11.94	-5.21	4.29	-3.96	-0.62	6552	110
rs-pc11	reference south	42.0	49.0	-17.60	-6.41	6.38	-3.97	2.98	6513	-13.89	-6.05	4.98	-4.87	-0.56	6552	119
tn-pc03	test north	35.0	37.0	-17.00	-6.42	6.27	-4.42	2.45	6520	-13.01	-6.03	4.75	-5.02	-0.73	6552	117
tn-pc04	test north	43.0	46.0	-14.79	-5.80	5.70	-3.18	1.59	6533	-12.16	-5.57	4.50	-4.35	-0.68	6552	110
tn-pc05	test north	32.0	36.0	-17.64	-6.99	6.39	-6.33	2.26	6545	-13.58	-6.38	4.93	-5.64	-0.62	6552	127
tn-pc06	test north	37.0	37.0	-18.30	-7.12	6.62	-7.22	2.16	6538	-14.43	-6.74	5.02	-6.01	-0.79	6548	124
tn-pc15	test north	48.0	51.0	-18.25	-7.39	6.06	-5.74	1.81	6540	-13.81	-6.08	4.90	-4.77	-0.70	6552	140
ts-pc07	test south	24.0	42.0	-17.38	-6.94	6.47	-6.11	2.02	6546	-13.93	-6.53	5.00	-5.57	-0.73	6552	122
ts-pc08	test south	15.0	46.0	-19.19	-7.21	7.04	-7.58	7.07	6550	-14.71	-6.63	5.24	-6.01	-0.48	6552	126
ts-pc12	test south	50.0	52.0	-18.16	-6.64	6.49	-5.31	5.13	6550	-13.47	-6.13	4.88	-4.97	-0.62	6552	117
ts-pc13	test south	43.0	44.0	-16.00	-6.23	5.90	-5.36	1.43	6536	-12.53	-5.99	4.46	-5.09	-0.90	6552	110
ts-pc14	test south	46.0	51.0	-18.16	-7.11	6.64	-6.77	3.30	6523	-14.47	-6.71	5.16	-5.95	-0.68	6552	127

direction. While air temperature is an important factor influencing soil temperatures (Shur and Jorgenson 2007), particularly in areas of continuous permafrost, other factors, including edaphic factors (Nossov et al. 2013), such as surface organic thickness, also affect soil temperature. Surface organic layers insulate underlying soils from the atmosphere; soils with thick surface organic layers tend to have more stable temperatures, and remain cooler in the summer and warmer in the winter, than soils with thin surface organic layers. For instance, plot ts-pc08 has the thinnest cumulative organic thickness in the active layer (15 cm) when compared to the other 15 plots (mean cumulative thickness. 42.8 cm). This plot also had the lowest and highest minimum and maximum soil temperatures at 30 cm during the freeze period, respectively, and the greatest variability in 30 cm soil temperature during the freeze period as measured by standard deviation of the mean (Table 6).

Cumulative organic thickness is not the only factor affecting soil temperatures. Soil temperatures at any given location and time are influenced by air temperature, insolation, surface albedo, surface organic thickness, vegetation, topography, soil moisture, and snow depth (Jorgenson et al. 2010, Zhang 2005). Of these factors, the CD5 Permafrost Monitoring study design controls for vegetation type, micro-topography, and soil moisture by placing plots, to the extent possible, in wet sedge or wet sedge willow tundra in low-centered polygons. It should be noted that the wet end of the soil moisture gradient commonly extends into areas where soils are not only saturated but are also continuously inundated by several centimeters of water; the presence of surface water has major implications for energy exchange. Measuring insolation and surface albedo are beyond the scope of this study. Snow depth and surface organic thickness are included in the monitoring program and the effects of these environmental factors on the soil temperatures are discussed below.

Snow surface has a high albedo that leads to a reduction in absorbed solar energy at the Earth's surface. Snow also insulates the ground surface from fluctuations in air temperature during the winter months. In general, sites with deeper snow throughout the winter tend to have more stable and generally warmer soil temperatures than sites with a shallow snowpack. For instance, plot rs-pc10 had the deepest late winter snow depth at the Hobo Installation (Table 3 and 6), and also had the warmest mean soil temperatures during the freeze period at both 30 and 100 cm. In contrast, the plot with the shallowest late winter snow depth, plot rn-pc02, had the third-coldest 30 cm and the coldest 100 cm mean soil temperatures during the freeze period. These two plots are also the most southerly, and second most northerly plots, respectively, and the role of regional air temperature gradients likely also affects the soil temperatures at these sites.

While snow depth helps to explain variability in soil temperature during the winter months, the relationship is not linear and other factors are also involved. Two of the three plots with the warmest mean 100 cm soil temperatures (Table 5) during the freezing season (rn-pc16 and rs-pc10) also had deep snowpacks in late winter (≥322 mm, Table 3), while plot tn-pc04, was moderately deep (269–290 mm). Similarly, two of the three plots with the coldest mean 100 cm soil temperatures (Table 6) during the freezing season (tn-pc15 and rn-pc02) also had shallow snow depth in late winter, while the snow depth at plot ts-pc08 was deep (≥322 mm, Table 3). Plot ts-pc08 was also the only plot located on a slightly convex polygon rim in an area of deep low-centered polygons and likely experiences colder soil temperatures during the freezing period because of its exposed micro-topographic position, despite a deeper late winter snow depth. The timing and rate of accumulation of snowfall in early winter are also important factors affecting soil temperatures during the freezing period (Zhang 2005). Early onset of snow would provide an earlier insulating effect resulting in warmer soils later in the winter. Additionally, a maximum snow depth achieved earlier in the winter would provide greater insulation during the coldest periods in February and March. During the winter of 2014–2015 the deepest snow depths occurred in April, after the coldest air temperatures (Figure 8).

The relationship between soil temperature and the variety of environmental factors that affect it necessitates a method that distills the complexity and facilitates the comparison of soil temperatures between plots. N-factor is one such method. N-factor is the ratio of seasonal degree-day sums near the soil surface to those in the air (Carlson 1952). N-factors integrate the complex relationships between near surface soil temperature, environmental factors (e.g., snow depth, surface organic thickness), and energy fluxes on an easily calculated numerical scale (Klene et al., 2001). N-factor values near one for a given day indicate a small difference between the near soil surface temperature and the air, whereas values near zero indicate soil temperatures colder than air temperature. Seasonal (i.e, thawing and freezing) cumulative daily n-factors provide a standardized means by which to compare the effects of air temperature on near surface soil temperature. Soils that are more insulated from the air by thick surficial organic deposits, snow, or surface water will have a lower n-factor, while the n-factor for soils that are less buffered from the air will be higher. Figures 15 and 16 display charts of daily cumulative thawing and freezing n-factor at 30 cm for each of 16 Permafrost Monitoring Plots by subarea, and Tables 5 and 6 present the maximum cumulative thawing and freezing n-factors at each plot. Plot rn-pc10 had the highest thawing n-factor (57) while ts-pc13 had the lowest (Table 5, Figure 15). This corresponds with the trends in thaw season soil temperature; these two plots also had the warmest and coldest mean soil temperature at 30 cm during the thaw season. Plots in reference area south consistently had some of the highest thawing n-factors overall, a trend likely related to the more southerly position of this reference area. The charts of cumulative n-factor also reveal plots with near surface soil temperatures that share very similar responses during the monitoring period. For instance, in Test Area North, plots tn-pc04 and tn-pc06 share very similar thawing n-factor trends, as do plots ts-pc14 and ts-pc07 in Test Area South. While most plots displayed a linear increase in thawing n-factor throughout the thaw season, plot tn-pc15 in Test Area North started out linear and then plateaued starting in early September and dropped below tn-pc05 soon thereafter. This trend is likely related to failure of the data logger at this plot as discussed above.

The charts of freezing n-factor show that the curves are more similar in slope and shape between plots during the freezing season than during the thaw season (Table 6, Figure 15). Plots rs-pc10, tn-pc04, and ts-pc13 had the lowest freezing n-factor at 30 cm, meaning that they were the most buffered from air temperatures. The plots had the first, second, and fourth warmest mean freezing season 30 cm soil temperatures, respectively. In addition, plots rs-pc10 and ts-pc13 had the first and third deepest late winter snow depths at the Hobo Installation, respectively (Table 3). Plots tn-pc15, rn-pc02, and tn-pc05 had the highest freezing n-factor. Of these three plots, rn-pc02 and tn-pc15 had the first and third shallowest late winter snow depths at the Hobo Installation, and the first and third coldest mean freezing season 30 cm soil temperatures, respectively. Plot tn-pc15 in Test Area North is the only plot displaying a slightly different trend in cumulative freezing n-factor. The freezing n-factor for this plot increases immediately at the beginning of October, while the other plots remain around zero until mid-January. This trend is likely related to failure of the data logger at this plot as discussed above.

DATA SUMMARIES BY REFERENCE AND TEST AREAS

Time-series of mean soil temperature and standard deviation at 30 and 100 cm aggregated by study area, and the mean daily air temperature at the Alpine Weather Station are presented in Figures 17–20. The time-series represent the soil temperatures at a broader spatial scale, which we used to compare the Test Areas (closer to the CD5 road) with the Reference Areas (farther from the road). In general, the aggregated soil temperature time-series follow a similar pattern as described above for the individual Permafrost Monitoring Plots. Reference Area South had the highest variability in temperature over the monitoring period, as indicated by the broad, overlapping standard deviation ribbons in Figure 18. Test Area South had the lowest variability in temperature over the monitoring period between Permafrost Monitoring Plots, as indicated by the relatively narrow, and less frequently overlapping standard deviation ribbons in Figure 20. Table 7 displays the summary statistics including annual mean, standard deviation and median values for each depth for the monitoring period aggregated by study area. Mean annual soil temperatures at

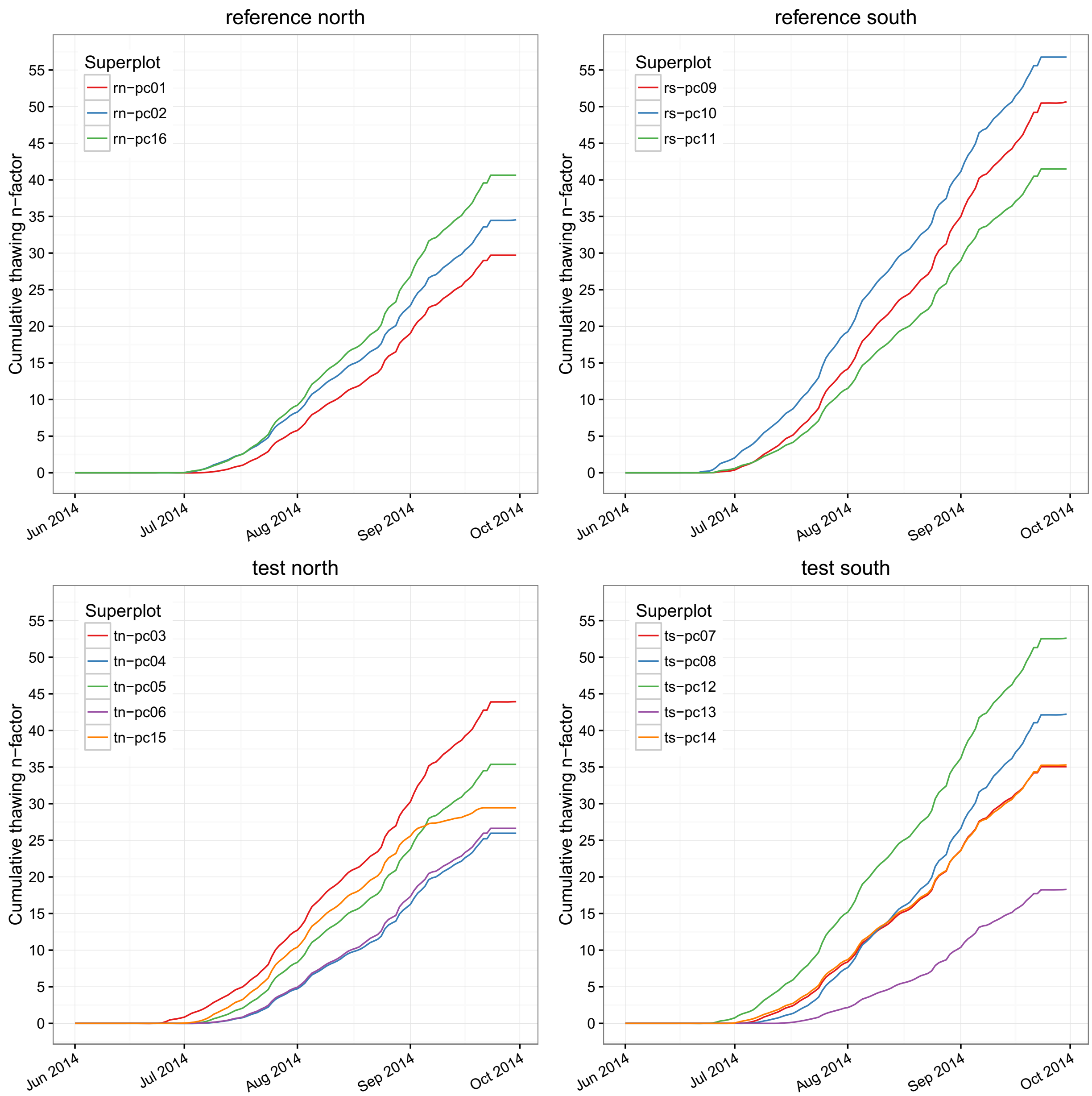

Figure 15. Daily cumulative thawing n-factor at 30 cm for each of 16 Permafrost Monitoring Plots by area, CD5 Habitat Monitoring Study, northern Alaska, June 2014–September 2014. Thawing n-factors displayed in this graph are calculated as the ratio of the thawing degree days in the soil to the thawing degree days of the air using the average of the Nuiqsut Airport and Alpine Weather Station average daily air temperature.

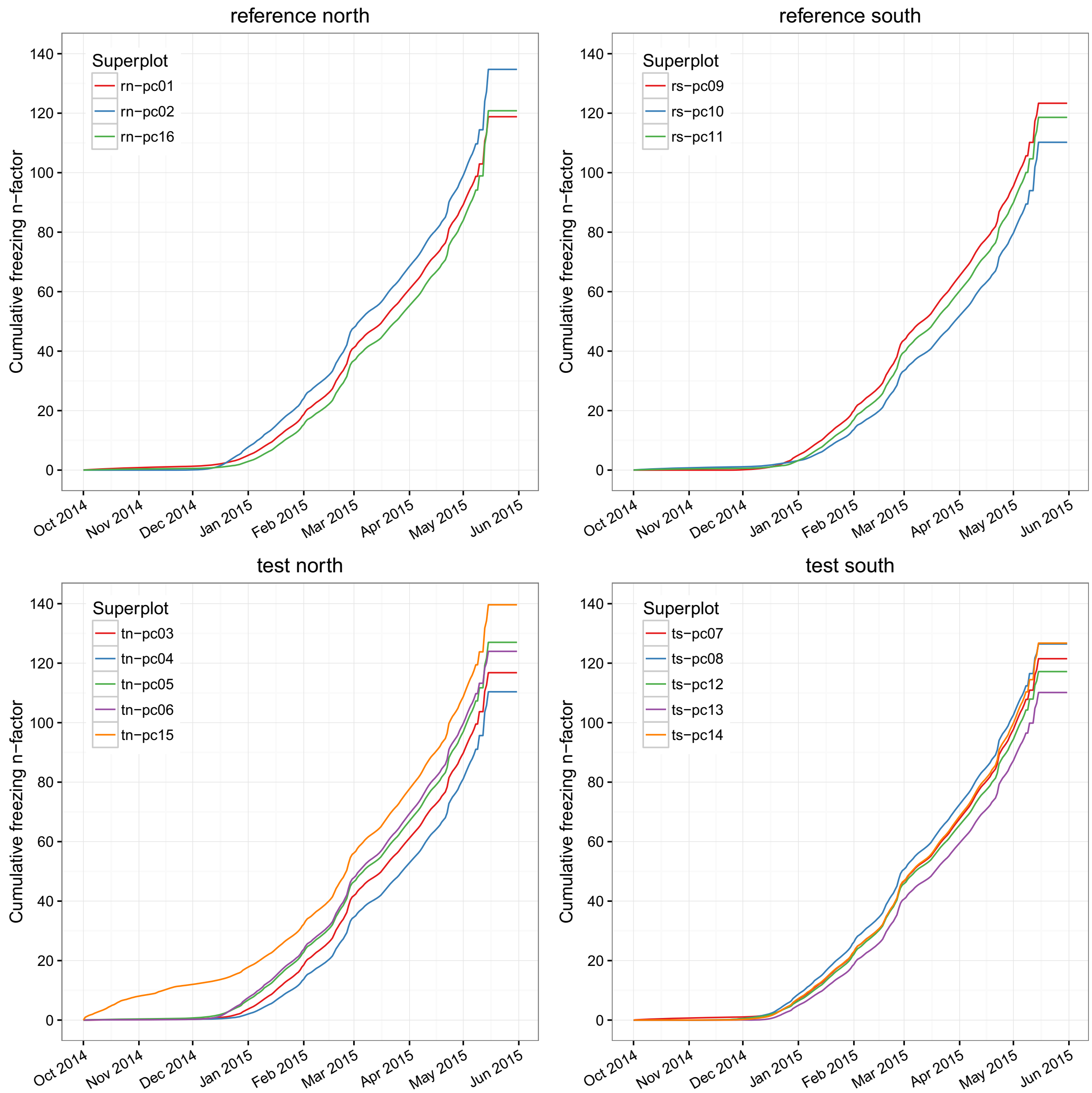

Figure 16. Daily cumulative freezing n-factor at 30 cm for each of 16 Permafrost Monitoring Plots by area, CD5 Habitat Monitoring Study, northern Alaska, October 2014–May 2015. Freezing n-factors displayed in this graph are calculated as the ratio of the freezing degree days in the soil to the freezing degree days of the air using the average of the Nuiqsut Airport and Alpine Weather Station average daily air temperature.

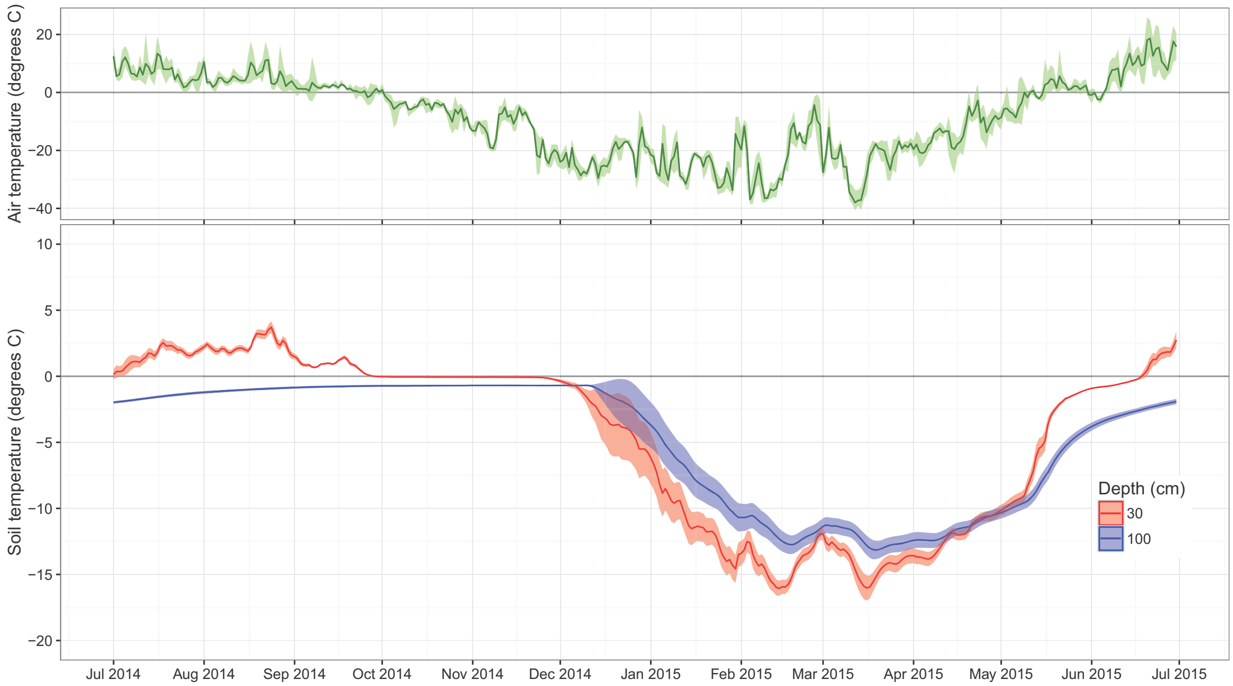

Figure 17. Time series of daily mean soil temperature and standard deviation at 30 cm and 100 cm for Reference Area North, and average daily minimum, mean and maximum air temperature, CD5 Habitat Monitoring Study, northern Alaska, July 2014–June 2015.

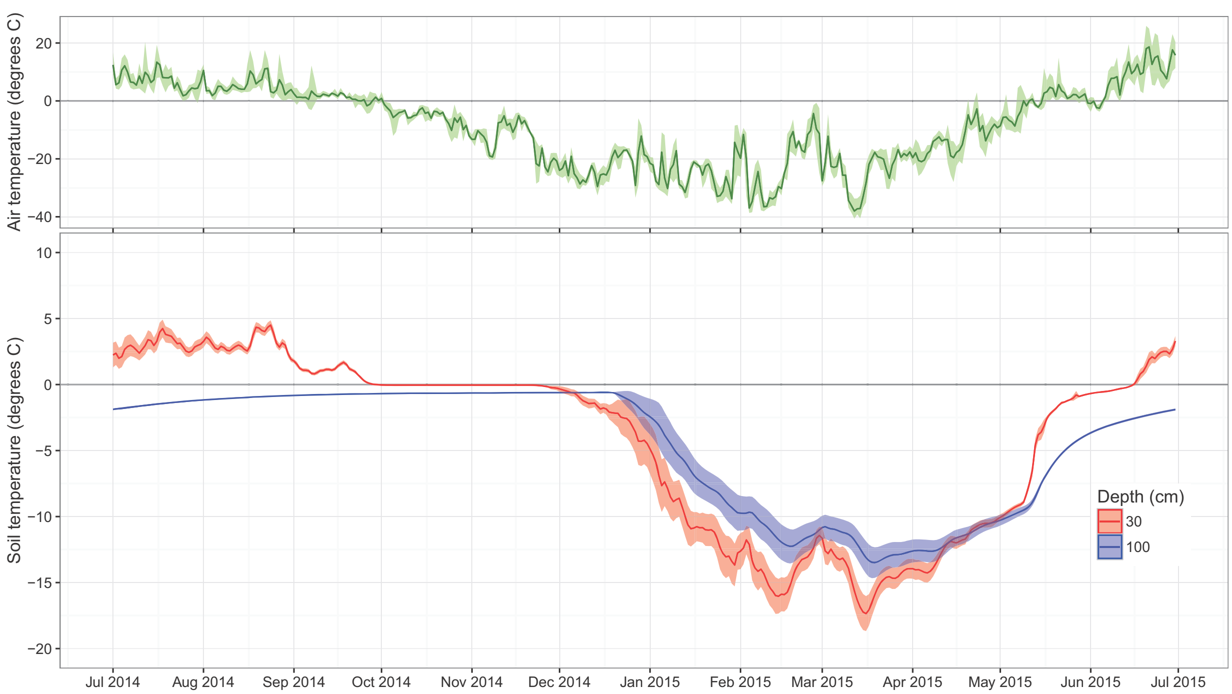

Figure 18. Time series of daily mean soil temperature and standard deviation at 30 cm and 100 cm for Reference Area South, and average daily minimum, mean and maximum air temperature, CD5 Habitat Monitoring Study, northern Alaska, July 2014–June 2015.

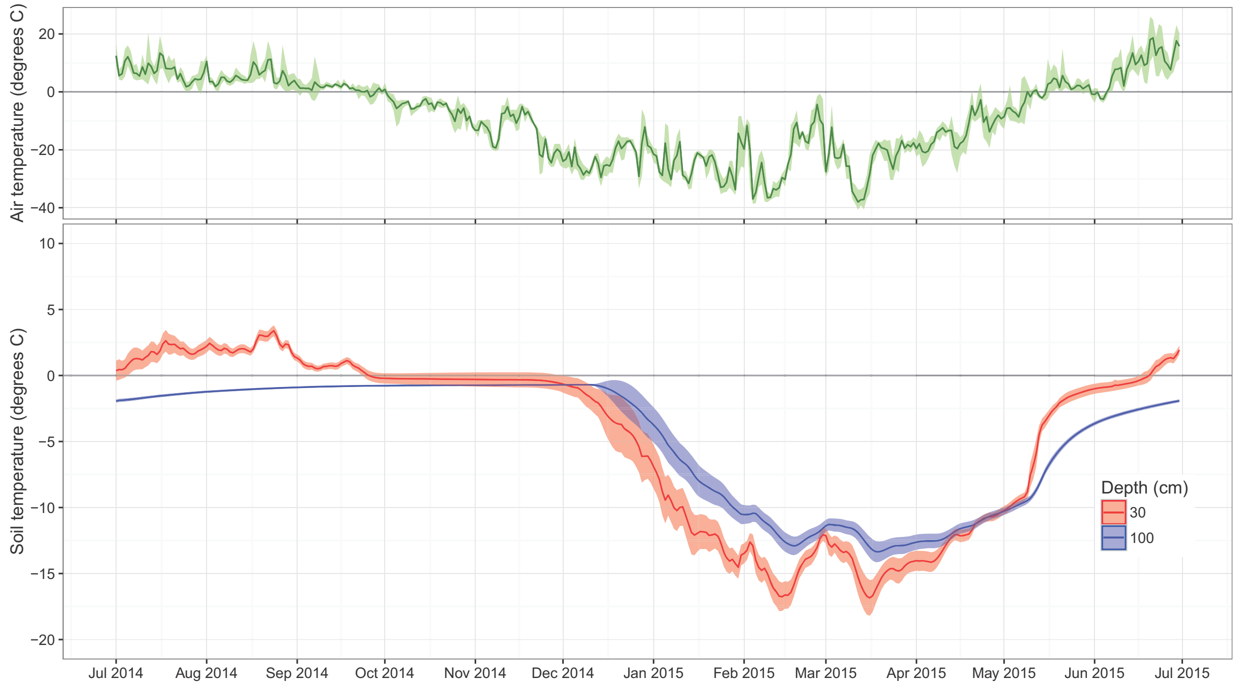

Figure 19. Time series of daily mean soil temperature and standard deviation at 30 cm and 100 cm for Test Area North, and average daily minimum, mean and maximum air temperature, and median weekly snow depth at the Alpine weather station, CD5 Habitat Monitoring Study, northern Alaska, July 2014–June 2015.

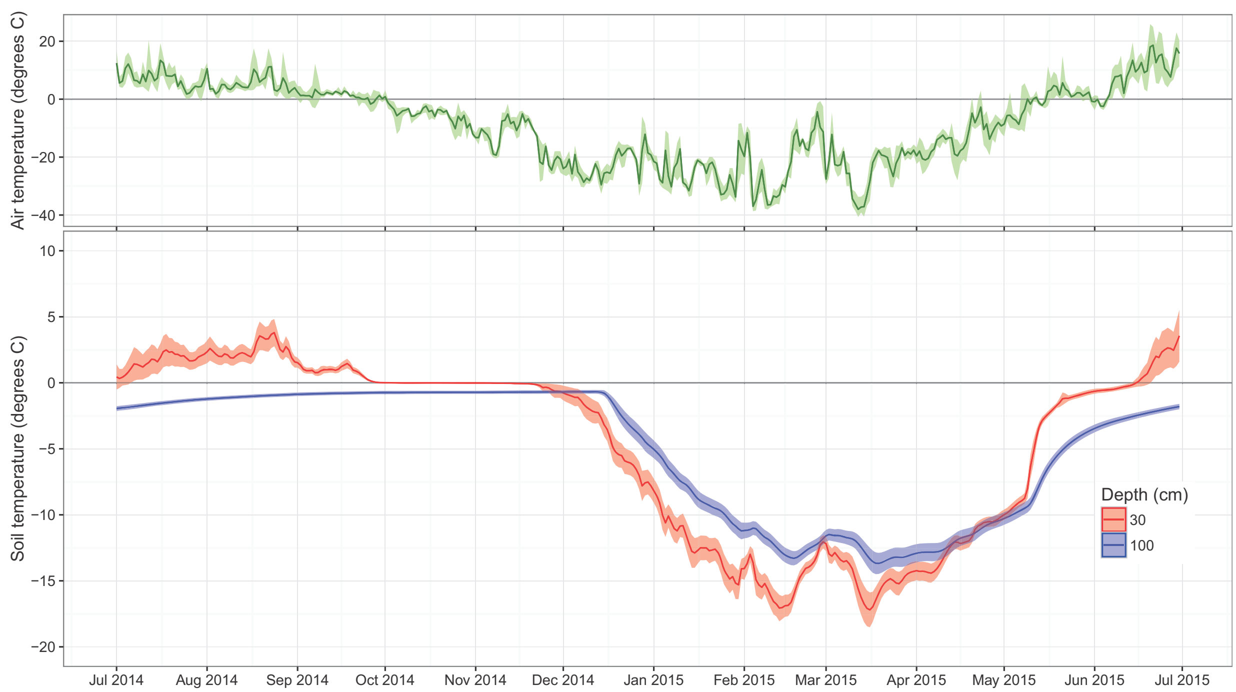

Figure 20. Time series of daily mean soil temperature and standard deviation at 30 cm and 100 cm for Test Area South, and average daily minimum, mean and maximum air temperature, CD5 Habitat Monitoring Study, northern Alaska, July 2014–June 2015.

Table 7. Soil temperature summary statistics at 30 cm and 100 cm, cumulative organic thickness (cm) within the active layer, and snow depth, density, and snow water equivalent (SWE) summarized by subarea, CD5 Habitat Monitoring Study, northern Alaska, July 2014–June 2015.

Area ID	Mean Temp at 30 cm (°C)	Std. Dev. Temp at 30 cm (°C)	Median Temp at 30 cm (°C)	Mean Temp at 100 cm (°C)	Std. Dev. Temp at 100 cm (°C)	Median Temp at 100 cm (°C)	Mean Cum. Org. Thickness in Active Layer (cm)
reference north	-4.48	6.39	-0.76	-4.91	4.72	-2.10	48.3
reference south	-4.08	6.63	-0.51	-4.68	4.69	-1.87	46.5
test north	-4.55	6.48	-0.59	-4.92	4.71	-2.13	39.0
test south	-4.70	6.76	-0.65	-5.07	4.87	-2.22	35.6

30 cm in the two Reference Areas were similar, ranging between -4.48 °C (± 6.39) at Reference Area North and -4.08 °C (±6.63) at Reference Area South. The mean temperature at 30 cm in Test Area North (-4.55 °C ± 6.48) was slightly colder than the two Reference Areas and Test Area South was the coldest subarea with a mean annual soil temperature at 30 cm of -4.70 °C (± 6.76) at 30 cm. The trend was similar for temperature at 100 cm with the warmest temperatures at Reference Area South, and the coldest at Test Area South. The slightly cooler temperatures in Test Area South may be attributed in part to the thinner cumulative organic thickness in this area (35.6 cm) compared to the other three areas (39.0–48.3 cm, Table 8), and the thin late winter snow depth (252 mm) compared to the other three (284–298 mm). Overall, the soil temperatures at 30 and 100 cm in all 4 areas were very similar. Test Area South, Test Area North, and Reference Area North were the most similar in mean annual soil temperature, occurring within approximately ±0.20 °C. Reference Area South was the warmest at both 30 and 100 cm and the most different from the other three, but the differences were still relatively small, ±0.72 °C in the most extreme case. Cumulative seasonal n-factors, normalize soil temperatures by relativizing them to air temperatures, allowing for more direct comparisons by season (Table 8, Figures 21 and 22). Any observed differences in n-factor between subareas can then be attributed to differences in environmental attributes that affect the thermal buffer between soil and air. During the thawing season, the most southerly subarea, Reference Area South, and the next most southerly subarea, Test Area South, had the highest and second highest cumulative thawing n-factors (50 and 41, respectively) (Figure 21). The two most northerly subareas followed a very similar trend earlier in the thawing season, but diverged later with Reference Area North ending the thaw season with a slightly higher cumulative thawing n-factor than Test Area North (35 and 33, respectively). The trends in thawing n-factor generally follow a latitudinal gradient, with higher thawing n-factors to the south, a trend that may in part be attributed to how n-factors were calculated; i.e., mean regional air temperatures rather than plot specific air temperatures. The use of mean regional air temperatures results in a slight overestimate of thawing n-factor to the south and underestimate to the north due to the higher average summer air temperatures and greater thawing degree days in the southern portion of the CD5 Study Area as measured at the Nuiqsut Airport compared to further north as measured at the Alpine Weather Station (Table 2, Figure 9). During the freezing season, the four subareas differed little in maximum cumulative freezing n-factor and shared similarly shaped cumulative freezing n-factor curves (Figure 22). This indicates that during the freezing season soils in the subareas are similarly affected by air temperature, and regional air temperature gradients between the southern and northern portions of the CD5 Study Area are less a factor in affecting soil temperatures than during the thaw period.

Table 8. Synthesis of key summary data by subarea, including cumulative organic thickness (cm), mean transect snow depth, mean annual soil temperature at 30 cm and 100 cm, and cumulative thawing and freezing n-factor, CD5 Habitat Monitoring Study, northern Alaska, July 2014–June 2015.

Area ID	Mean Cum. Org. Thickness in Active Layer (cm)	Mean Transect Snow Depth (mm)	Mean Temp at 30 cm (°C)	Mean Temp at 100 cm (°C)	Mean Cumulative Thawing n-factor	Mean Cumulative Freezing n-factor
reference north	48.3	284	-4.48	-4.91	35	125
reference south	46.5	286	-4.08	-4.68	50	117
test north	39.0	298	-4.55	-4.92	33	120
test south	35.6	252	-4.70	-5.07	41	120

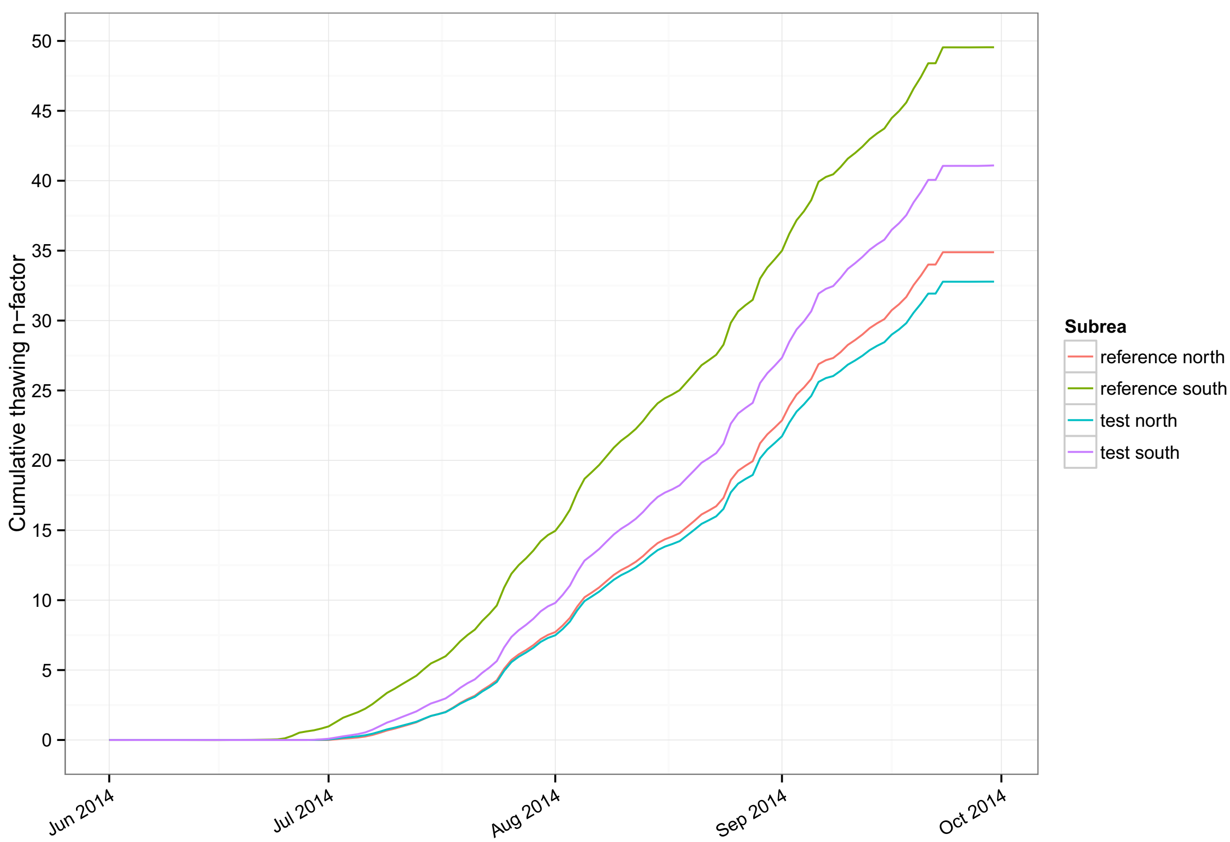

Figure 21. Average daily cumulative thawing n-factor at 30 cm for Permafrost Monitoring Plots in Reference Area North, Reference Area South, Test Area North, and Test Area South, CD5 Habitat Monitoring Study, northern Alaska, June 2014–September 2014. Thawing n-factors displayed in this graph are calculated as the ratio of the thawing degree days in the soil to the thawing degree days of the air using the average of the Nuiqsut Airport and Alpine Weather Station average daily air temperature.

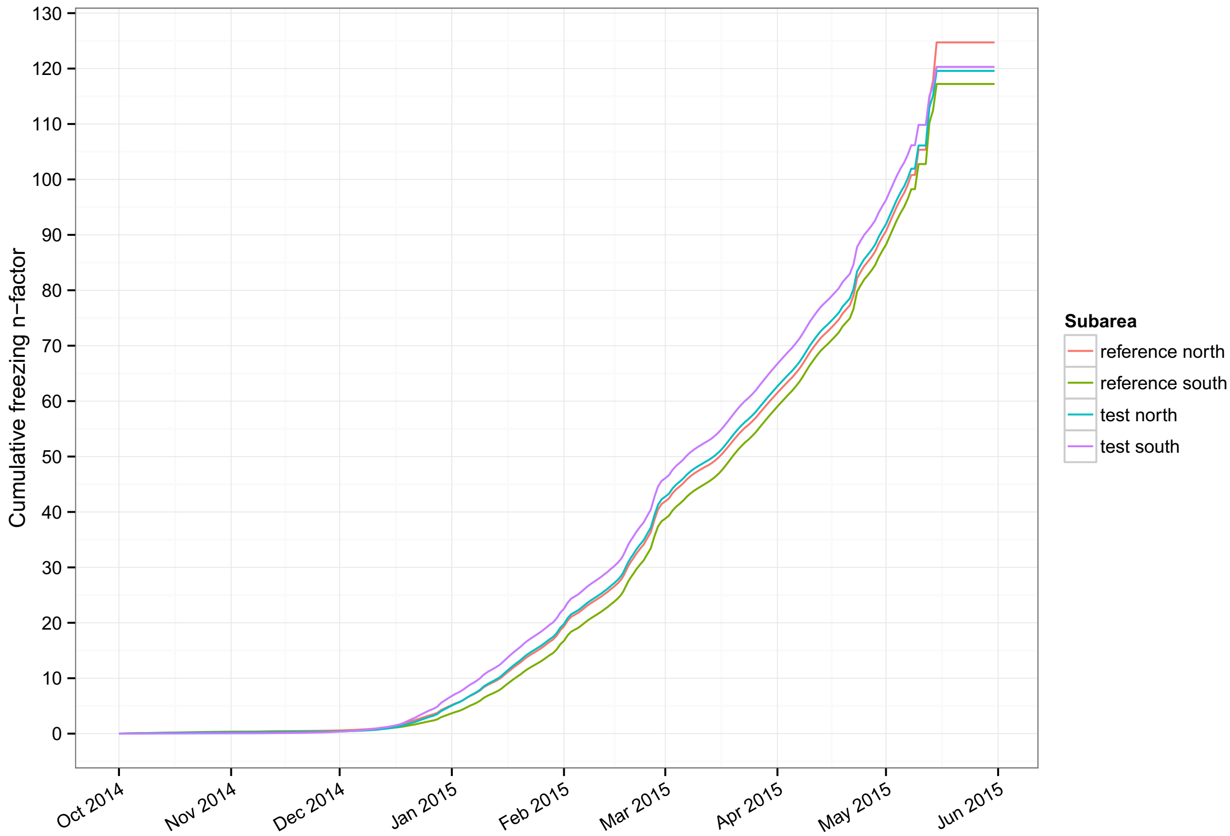

Figure 22. Average cumulative freezing n-factor at 30 cm for Permafrost Monitoring Plots in Reference Area North, Reference Area South, Test Area North, and Test Area South, CD5 Habitat Monitoring Study, northern Alaska, October 2014–May 2015. Freezing n-factors displayed in this graph are calculated as the ratio of the freezing degree days in the soil to the freezing degree days of the air using the average of the Nuiqsut Airport and Alpine Weather Station average daily air temperature.

LITERATURE CITED

ABR, Inc.—Environmental Research and Services and Michael Baker, Jr. Inc. (ABR and Baker). 2011. Assessment of the impacts of potential changes in sedimentation and erosion regime on the Colville River Delta related to the proposed CD5 Drill Site Development. Prepared for ConocoPhillips Alaska, Inc, Anchorage, Alaska. 83 pp.

ABR, Inc. Environmental Research and Services and Michael Baker, Jr. Inc. (ABR and Baker). 2013. Monitoring plan with an adaptive management strategy, CD5 development project. Prepared for ConocoPhillips Alaska, Inc, Anchorage, Alaska. 171 pp.

Arnborg, L., H. J. Walker, and J. Peippo. 1966. Water discharge in the Colville River, 1962. Geografiska Annaler, Series A, Physical Geography 48: 195–210.

Baker, Michael Jr. 2015. 2015 Colville River Delta spring breakup monitoring and hydrological assessment. Prepared for ConocoPhillips Alaska, Inc, Anchorage, Alaska. 250 pp.

Benson, C. S. and M. Sturm. 1993. Structure and wind transport of seasonal snow on the Arctic Slope of Alaska. Annals of Glaciology, 18, 261–267.

Carlson, H. 1952. Calculation of depth of thaw in frozen ground. Frost Action in Soils: A Symposium. Washington, DC: Highway Research Board Special Report 2, National Research Council. p 192-223.

Derry, J.E., D.L. Kane, M.R. Lilly, and H. Toniolo, 2009. Snow-Course Measurement Methods, North Slope, Alaska. December 2009, University of Alaska Fairbanks, Water and Environmental Research Center, Report Number INEWERC2009.07, Fairbanks, Alaska, 11 pp.

Karunaratne, K.C. and Burn, C.R. 2003. Freezing n-factors in discontinuous permafrost terrain, Takhini River, Yukon Territory, Canada. Pages 519–625 In: Phillips, Springman, & Arenson, eds. Proceedings of the Eighth International Conference on Permafrost, 21–25 JUly 2003, Zurich, Switzerland.

Klene, A.E, F.E. Nelson, N.I. Shiklomanov, and K.M. Hinkel. 2001. The n-factor in natural landscapes: variability of air and soil-surface temperatures, Kuparuk River Basin, Alaska, U.S.A. Arctic, Antarctic, and Alpine Research. 33:140–148.

Jorgenson, M.T., Romanovsky, V.E., Harden, J., Shur, Y, O'Donnell, J., Schuur E.A.G., Kanevskiy, M., and Marchenko, S.S. 2010. Resilience and vulnerability of permafrost to climate change. Canadian Journal of Forest Research. 40(7): 1219-1236.

Jorgenson T, K. Yoshikawa, M. Kanevskiy, Y. Shur, V. Romanovsky, S. Marchenko, G. Grosse, J. Brown, and B. Jones. 2008. Permafrost Characteristics of Alaska - A new permafrost map of Alaska. Institute of Northern Engineering, University of Alaska Fairbanks. Ninth International Conference on Permafrost.

National Centers for Environmental Information (NCEI). 2010. 1981–2010 U.S. Climate Normals. U.S. Department of Commerce. https://www.ncdc.noaa.gov/data-access/land-based-station-data/land-based-datasets/climate-normals/1981-2010-normals-data, accessed November, 2015.

National Centers for Environmental Information (NCEI). 2015. Global Historical Climatology Network—Daily. U.S. Department of Commerce. http://lwf.ncdc.noaa.gov/oa/climate/ghcn-daily/index.php, accessed November 2015.

Nossov, D.R., Jorgenson, M.T., Kielland, K., and Kanevskiy, M.Z. 2013. Edaphic and microclimatic controls over permafrost response to fire in interior Alaska. Environmental Research Letters 8: 1–12.

Outcalt, S.I,, F.E. Nelson, and K.M., Hinkel. 1990. The zero-curtain effect: heat and mass transfer across an isothermal region in freezing soil. Water Resources Research. 26:1509–1516.

PostgreSQL Global Development Group. 2015. PostgreSQL: A powerful, open source object-relational database system. http://www.postgresql.org/

R Core Team. 2015. R: A language and environment for statistical computing. R Foundation for Statistical Computing, Vienna, Austria. http://www.R-project.org/

Shur, Y. L. and Jorgenson, M. T. 2007, Patterns of permafrost formation and degradation in relation to climate and ecosystems. Permafrost Periglac. Process., 18: 7–19.

Sturm, M., J. Holmgren, J. P. McFadden, G. E. Liston, F. S. Chapin III, and C. H. Racine. 2001. Snow-shrub interactions in Arctic tundra: a hypothesis with climatic implications. Journal of Climate, 14(3), 336–344.

Sturm, M., B. Taras, G. E. Liston, C. Derksen, Tobias Jonas, Jon Lea, 2010. Estimating Snow Water Equivalent Using Snow Depth Data and Climate Classes. Journal of Hydrometeorology, 11, 1380–1394.

Viereck, L. A., C. T. Dyrness, A. R. Batten, and K. J. Wenzlick. 1992. The Alaska Vegetation Classification. Pacific Northwest Research Station, U. S. Forest Service, Portland, OR. General Technical Report PNW-GTR-286. 278 pp.

Walker, D. A. 1983. A hierarchical tundra vegetation classification especially designed for mapping in northern Alaska. Pages 1332–1337 in Permafrost Fourth International Conference Proceedings. Univ. of Alaska Fairbanks, AK. National Academy Press, Washington, DC.

Walker, H. J. 1976. Depositional environments in the Colville River Delta. Pages C1–C22 in T. P. Moller, ed., Recent and ancient sedimentary environments in Alaska. Alaska Geological Society, Anchorage, AK.

Wells, A.F., Macander, M.J., Swingley, C.S., Cater, T.C., Christopherson, T., Kade, A.N., Morgan, T.C., and St. Lawrence, W.F. 2014. 2014 Habitat monitoring and assessment, CD5 development project. Prepared for ConocoPhillips Alaska, Inc, Anchorage, Alaska. 183 pp.

Wells, A.F., Swingley, C.S., Christopherson, T. 2015. 2014 Habitat Monitoring and Assessment: Permafrost Component, CD5 development project. Prepared for ConocoPhillips Alaska, Inc, Anchorage, Alaska. 55 pp.

Wickham, H. 2009. ggplot2: elegant graphics for data analysis. Springer New York. 212pp. http://had.co.nz/ggplot2/book

Woo, M-K. 1997. A guide for ground based measurement of the arctic snow cover. Canadian Snow Data CD, Meteorological Service of Canada, Downsview, Ontario, 30 pp.

Zhang, T. 2005. Influence of the seasonal snow cover on the ground thermal regime: an overview. Reviews of Geophysics. 43: 1–23.

Appendix A-1. Alpine weather station weekly snow depth summary stats from September 2014–June 2015, CD5 Habitat Monitoring Study, northern Alaska, July 2014–June 2015.

Week Beginning On	Min. Weekly Snow Depth (mm)	Mean Weekly Snow Depth (mm)	St. Dev. Weekly Snow Depth (mm)	Median Weekly Snow Depth (mm)	Max. Weekly Snow Depth (mm)
2014-09-01	0	0	0	0	0
2014-09-08	0	0	0	0	0
2014-09-15	0	0	0	0	0
2014-09-22	0	0	0	0	0
2014-09-29	0	1	3	0	15
2014-10-06	1	42	20	47	92
2014-10-13	51	67	10	69	120
2014-10-20	65	110	34	121	166
2014-10-27	132	143	7	143	167
2014-11-03	130	140	4	139	157
2014-11-10	119	133	6	136	141
2014-11-17	119	143	7	145	159
2014-11-24	138	147	4	149	154
2014-12-01	114	134	8	137	147
2014-12-08	107	135	16	144	161
2014-12-15	140	145	2	145	151
2014-12-22	136	146	5	147	172
2014-12-29	95	139	10	139	166
2015-01-05	92	124	16	123	150
2015-01-12	121	143	15	145	290
2015-01-19	133	148	10	146	193
2015-01-26	141	154	15	146	248
2015-02-02	157	160	2	160	170
2015-02-09	157	159	1	160	161
2015-02-16	159	186	22	177	218
2015-02-23	154	183	34	163	348
2015-03-02	221	243	7	244	274
2015-03-09	214	244	6	244	279
2015-03-16	214	246	13	245	318
2015-03-23	229	246	7	245	314
2015-03-30	232	295	28	309	355
2015-04-06	305	323	21	311	380
2015-04-13	299	321	19	309	357
2015-04-20	292	344	21	356	363
2015-04-27	348	360	3	361	365
2015-05-04	337	356	9	359	383
2015-05-11	246	294	25	293	338
2015-05-18	0	127	85	151	245
2015-05-25	0	0	0	0	0
2015-06-01	0	0	0	0	0
2015-06-08	0	0	0	0	0
2015-06-15	0	0	0	0	0
2015-06-22	0	0	0	0	0

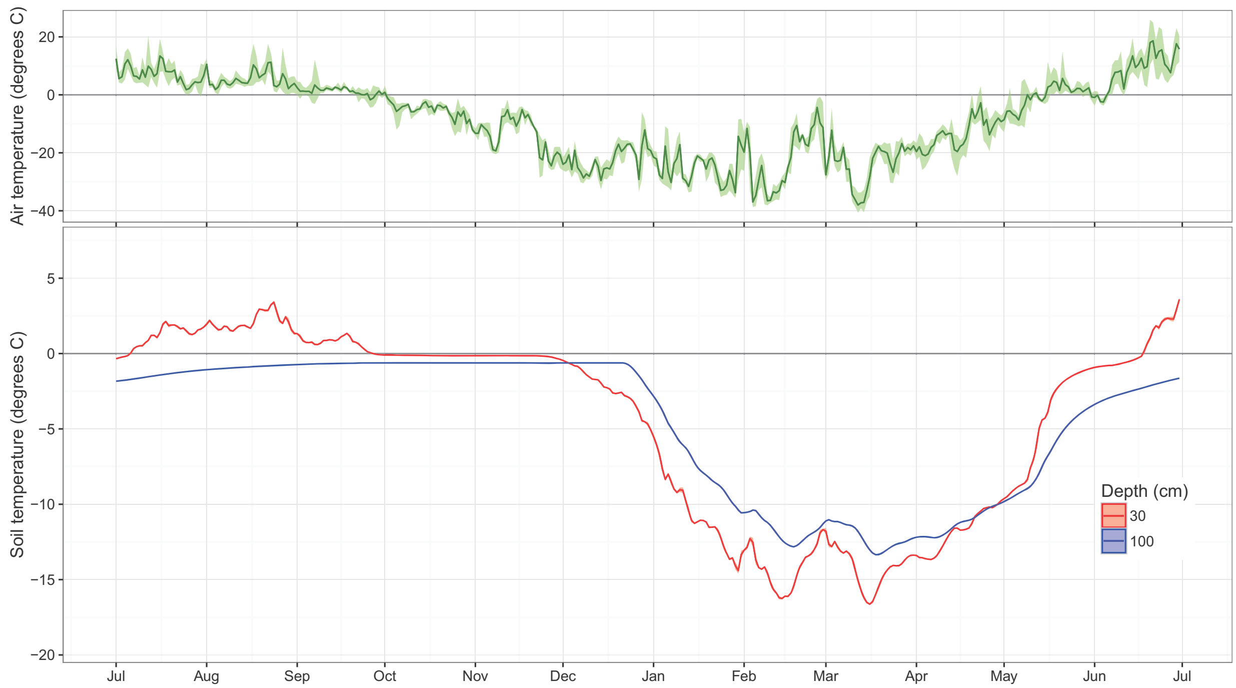

Appendix B-1. Time series of daily median soil temperature at 30 cm and 100 cm at Permafrost Monitoring Plot rn-pc01 (hobo serial number 10392122) and average daily air temperature at the Alpine weather station, CD5 Habitat Monitoring Study, northern Alaska, July 2014–June 2015.

Appendix B-2. Time series of daily median soil temperature at 30 cm and 100 cm at Permafrost Monitoring Plot rn-pc02 (hobo serial number 10392123) and average daily air temperature at the Alpine weather station, CD5 Habitat Monitoring Study, northern Alaska, July 2014–June 2015.

Appendix B-3. Time series of daily median soil temperature at 30 cm and 100 cm at Permafrost Monitoring Plot rn-pc16 (hobo serial number 10392137) and average daily air temperature at the Alpine weather station, CD5 Habitat Monitoring Study, northern Alaska, July 2014–June 2015.

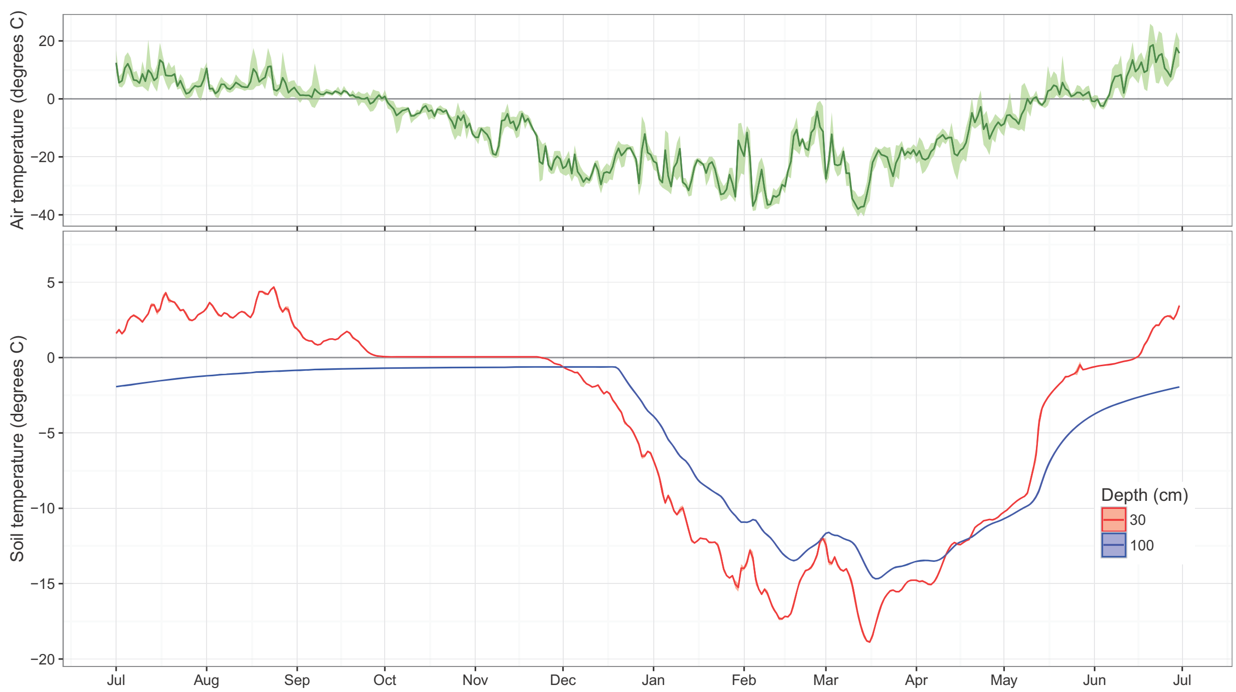

Appendix B-4. Time series of daily median soil temperature at 30 cm and 100 cm at Permafrost Monitoring Plot rs-pc09 (hobo serial number 10392130) and average daily air temperature at the Alpine weather station, CD5 Habitat Monitoring Study, northern Alaska, July 2014–June 2015.

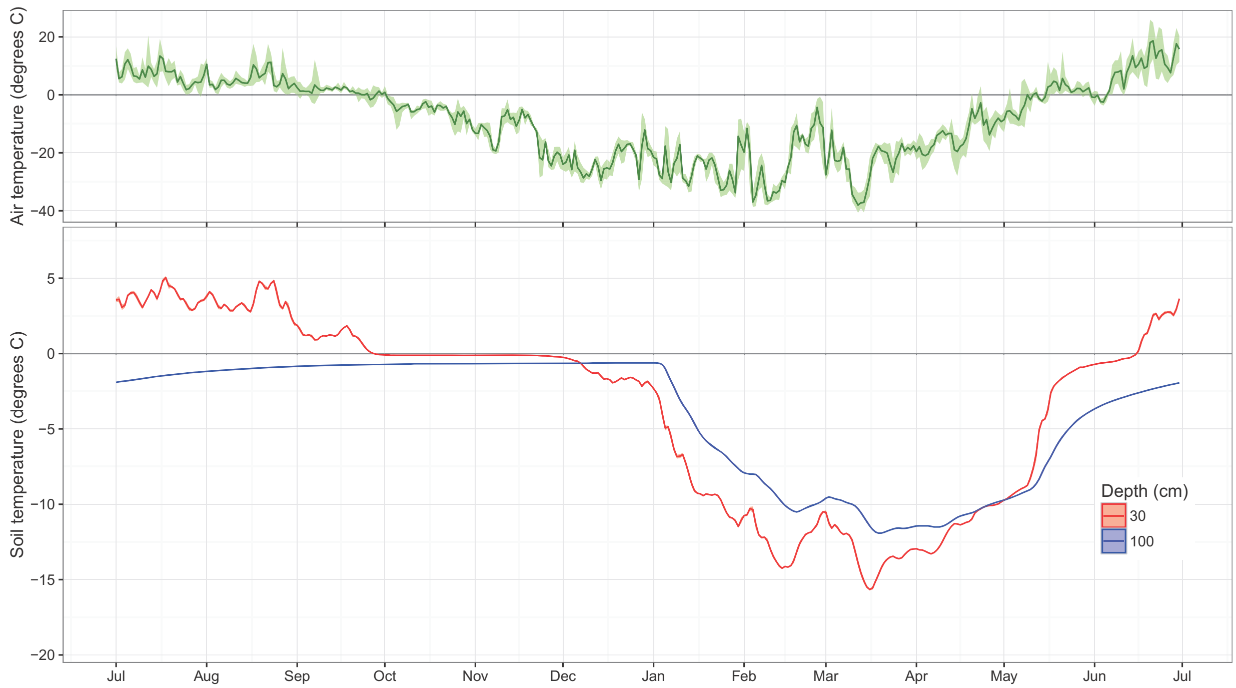

Appendix B-5. Time series of daily median soil temperature at 30 cm and 100 cm at Permafrost Monitoring Plot rs-pc10 (hobo serial number 10392131) and average daily air temperature at the Alpine weather station, CD5 Habitat Monitoring Study, northern Alaska, July 2014–June 2015.

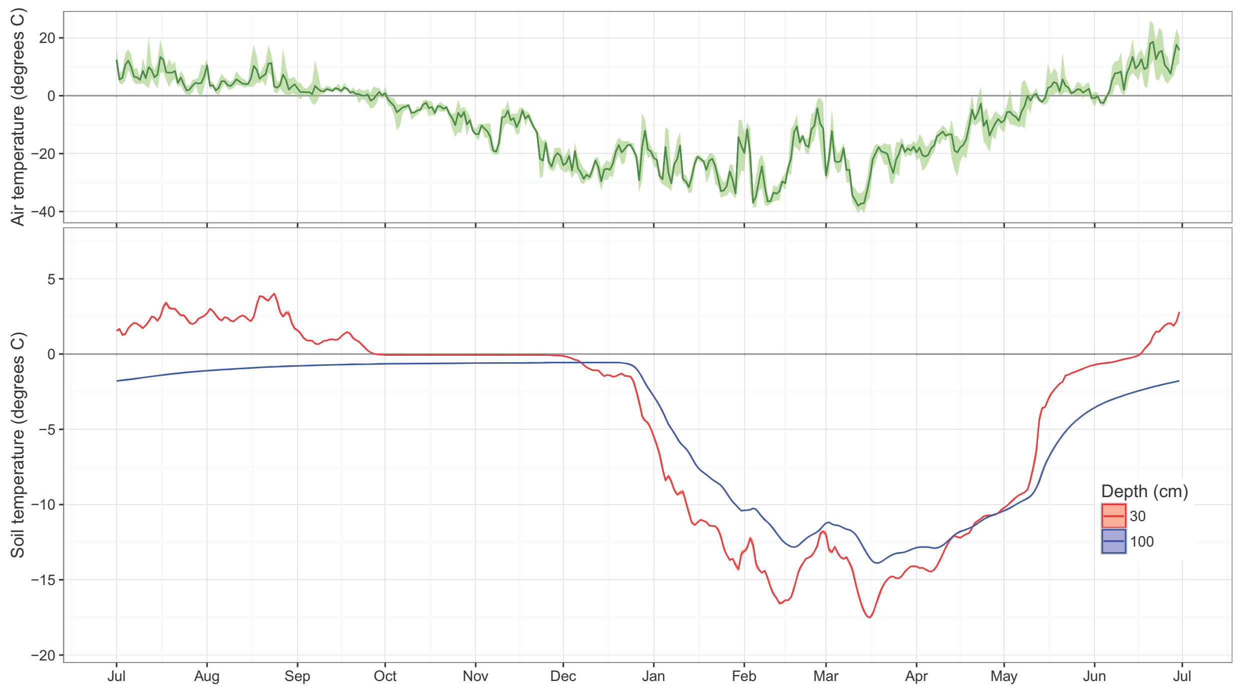

Appendix B-6. Time series of daily median soil temperature at 30 cm and 100 cm at Permafrost Monitoring Plot rs-pc11 (hobo serial number 10392132) and average daily air temperature at the Alpine weather station, CD5 Habitat Monitoring Study, northern Alaska, July 2014–June 2015.

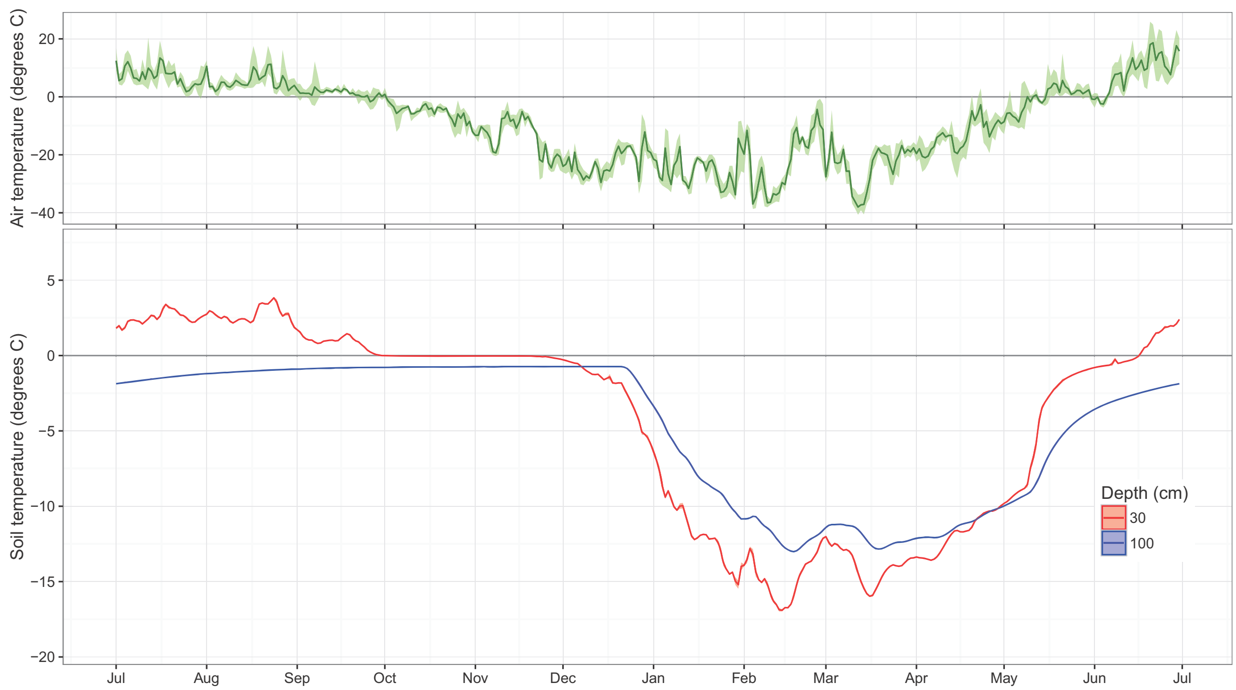

Appendix B-7. Time series of daily median soil temperature at 30 cm and 100 cm at Permafrost Monitoring Plot tn-pc03 (hobo serial number 10392124) and average daily air temperature at the Alpine weather station, CD5 Habitat Monitoring Study, northern Alaska, July 2014–June 2015.

Appendix B-8. Time series of daily median soil temperature at 30 cm and 100 cm at Permafrost Monitoring Plot tn-pc04 (hobo serial number 10392125) and average daily air temperature at the Alpine weather station, CD5 Habitat Monitoring Study, northern Alaska, July 2014–June 2015.

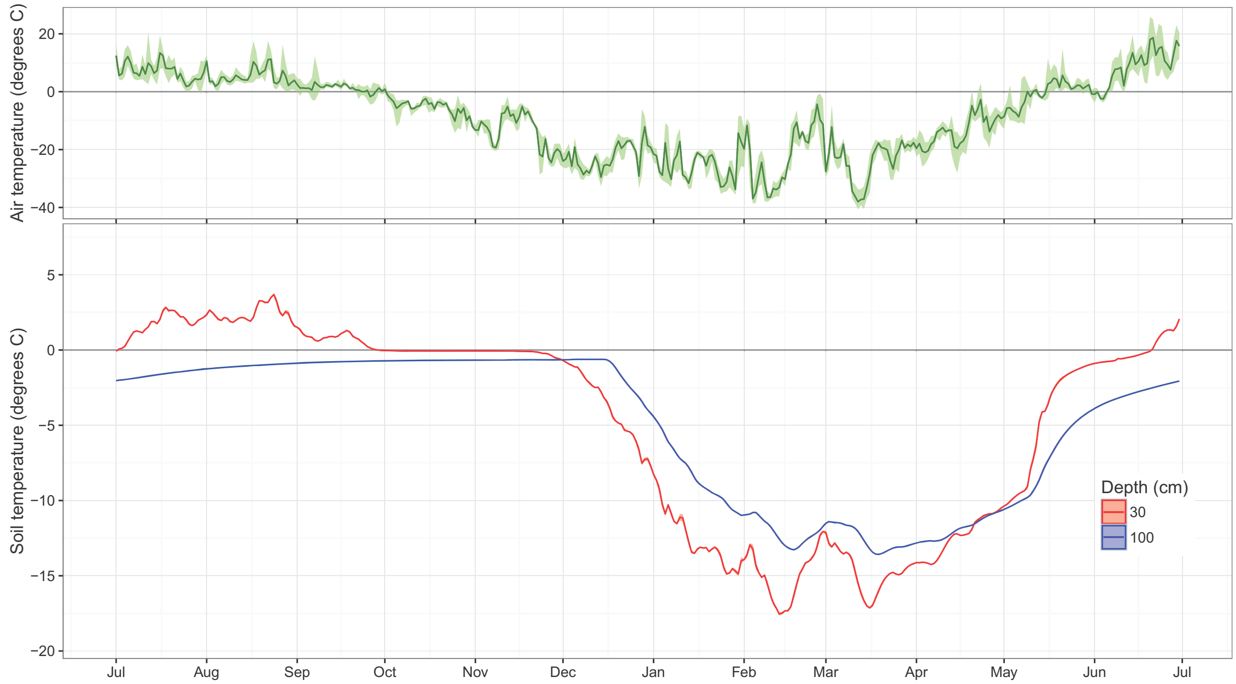

Appendix B-9. Time series of daily median soil temperature at 30 cm and 100 cm at Permafrost Monitoring Plot tn-pc05 (hobo serial number 10392126) and average daily air temperature at the Alpine weather station, CD5 Habitat Monitoring Study, northern Alaska, July 2014–June 2015.

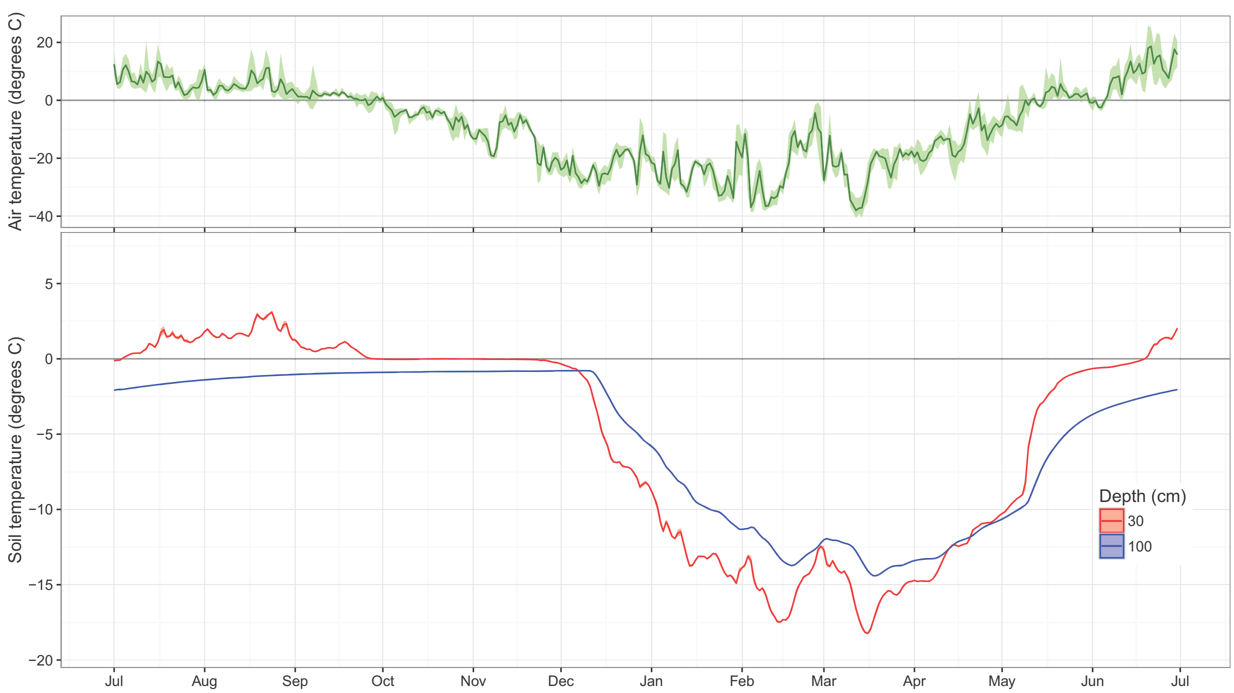

Appendix B-10. Time series of daily median soil temperature at 30 cm and 100 cm at Permafrost Monitoring Plot tn-pc06 (hobo serial number 10392127) and average daily air temperature at the Alpine weather station, CD5 Habitat Monitoring Study, northern Alaska, July 2014–June 2015.

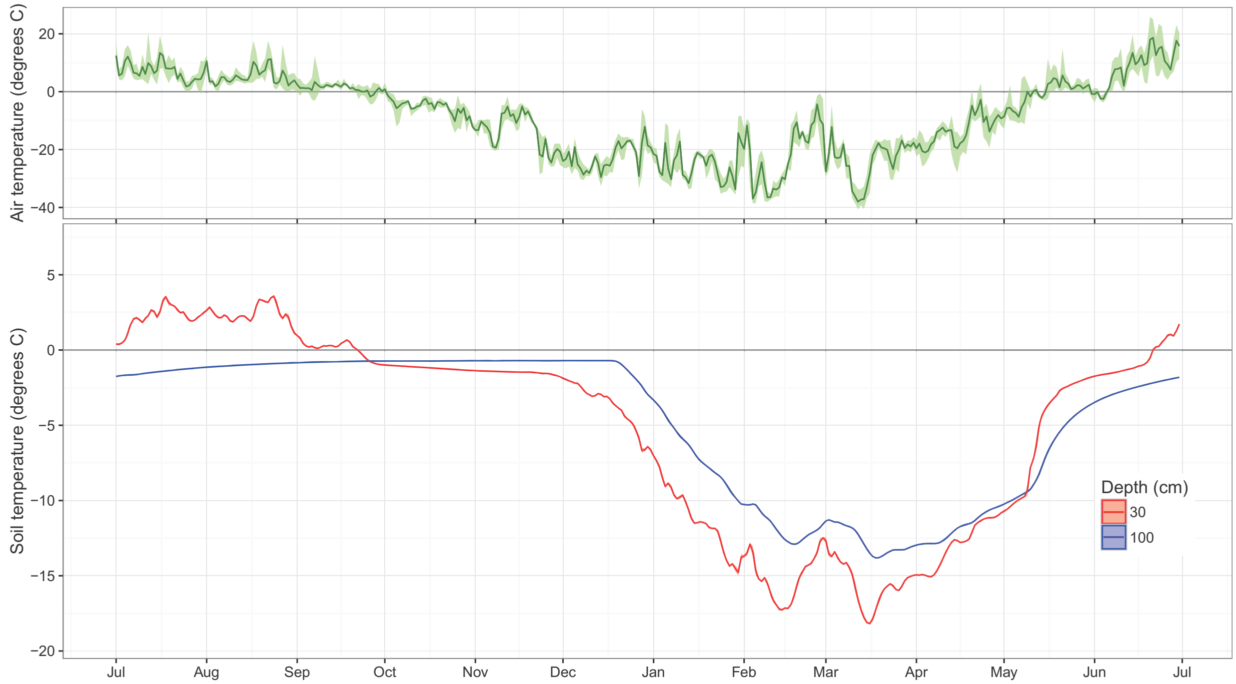

Appendix B-11. Time series of daily median soil temperature at 30 cm and 100 cm at Permafrost Monitoring Plot tn-pc15 (hobo serial number 10392136) and average daily air temperature at the Alpine weather station, CD5 Habitat Monitoring Study, northern Alaska, July 2014–June 2015.

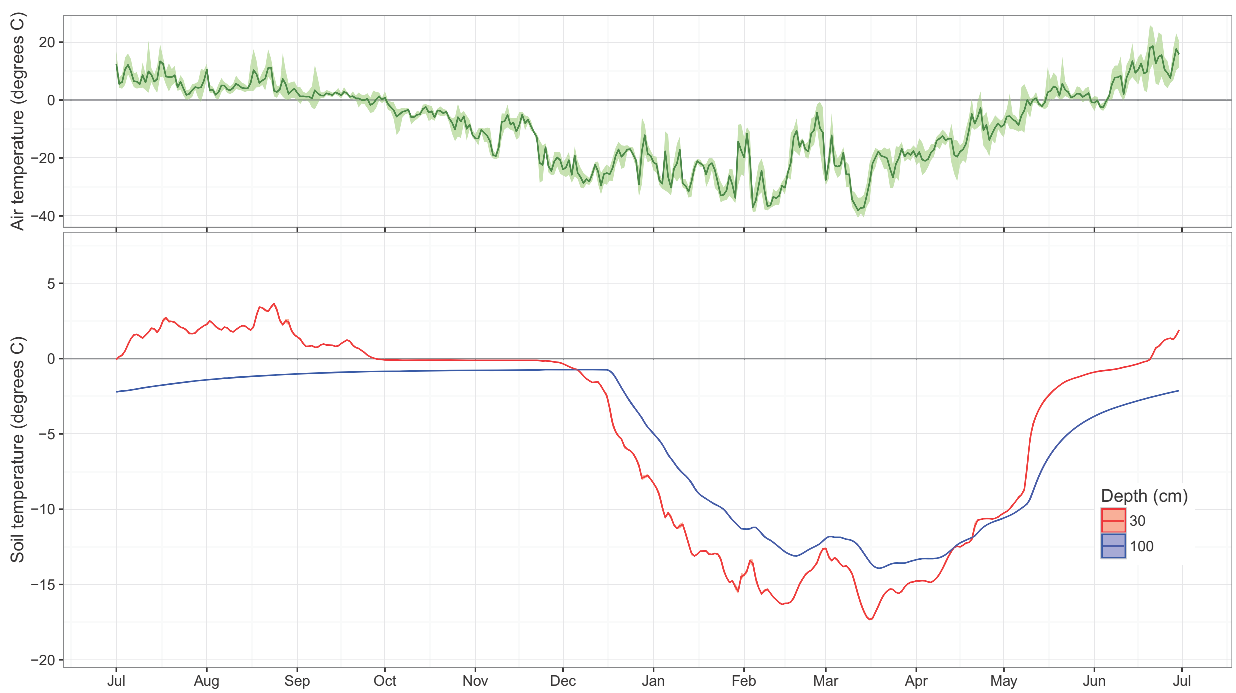

Appendix B-12. Time series of daily median soil temperature at 30 cm and 100 cm at Permafrost Monitoring Plot ts-pc07 (hobo serial number 10392128) and average daily air temperature at the Alpine weather station, CD5 Habitat Monitoring Study, northern Alaska, July 2014–June 2015.

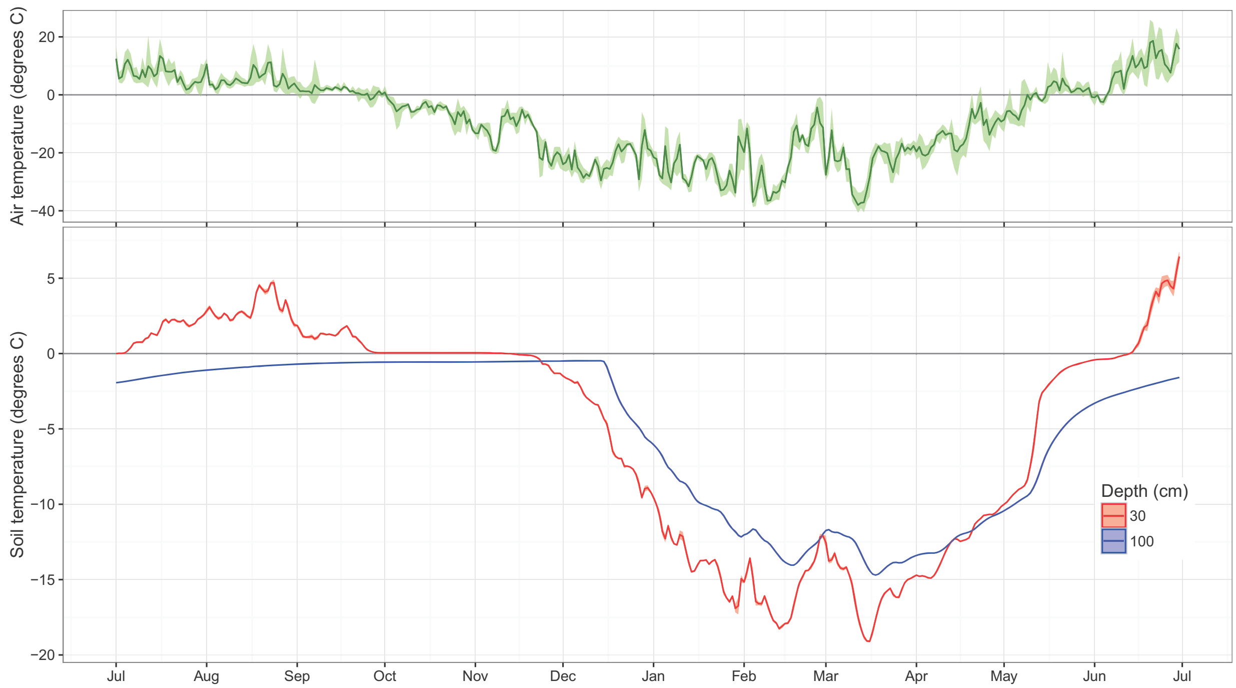

Appendix B-13. Time series of daily median soil temperature at 30 cm and 100 cm at Permafrost Monitoring Plot ts-pc08 (hobo serial number 10392129) and average daily air temperature at the Alpine weather station, CD5 Habitat Monitoring Study, northern Alaska, July 2014–June 2015.

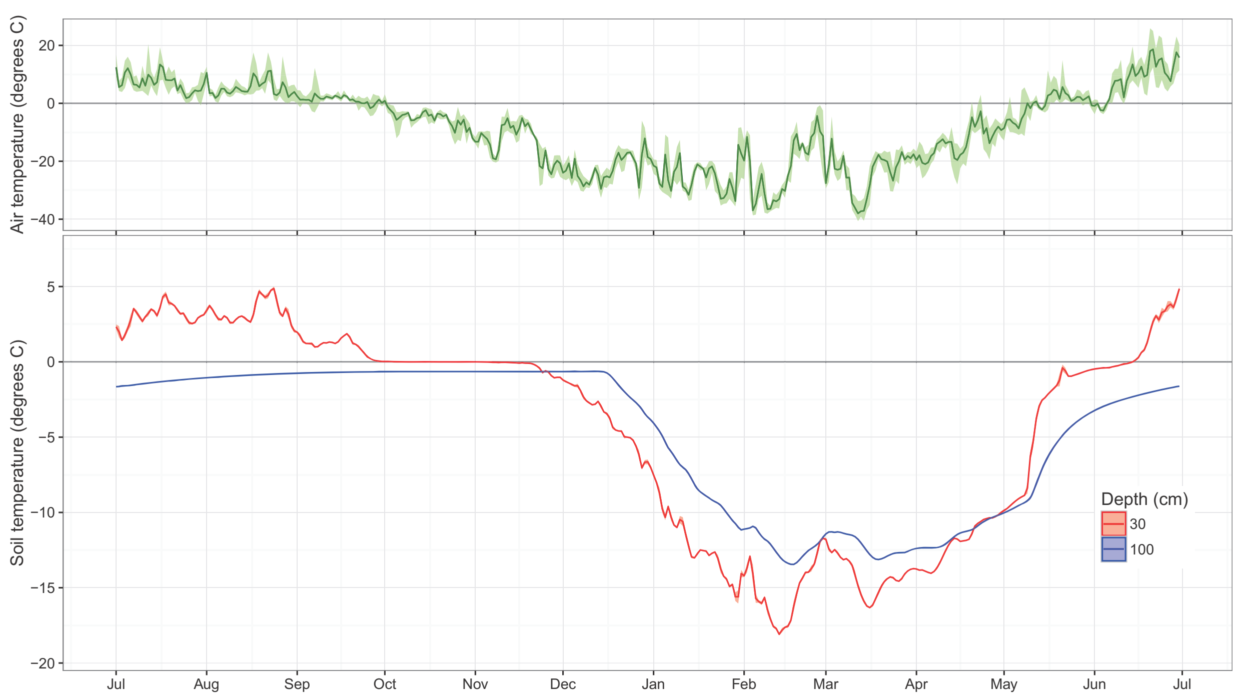

Appendix B-14. Time series of daily median soil temperature at 30 cm and 100 cm at Permafrost Monitoring Plot ts-pc12 (hobo serial number 10392133) and average daily air temperature at the Alpine weather station, CD5 Habitat Monitoring Study, northern Alaska, July 2014–June 2015.

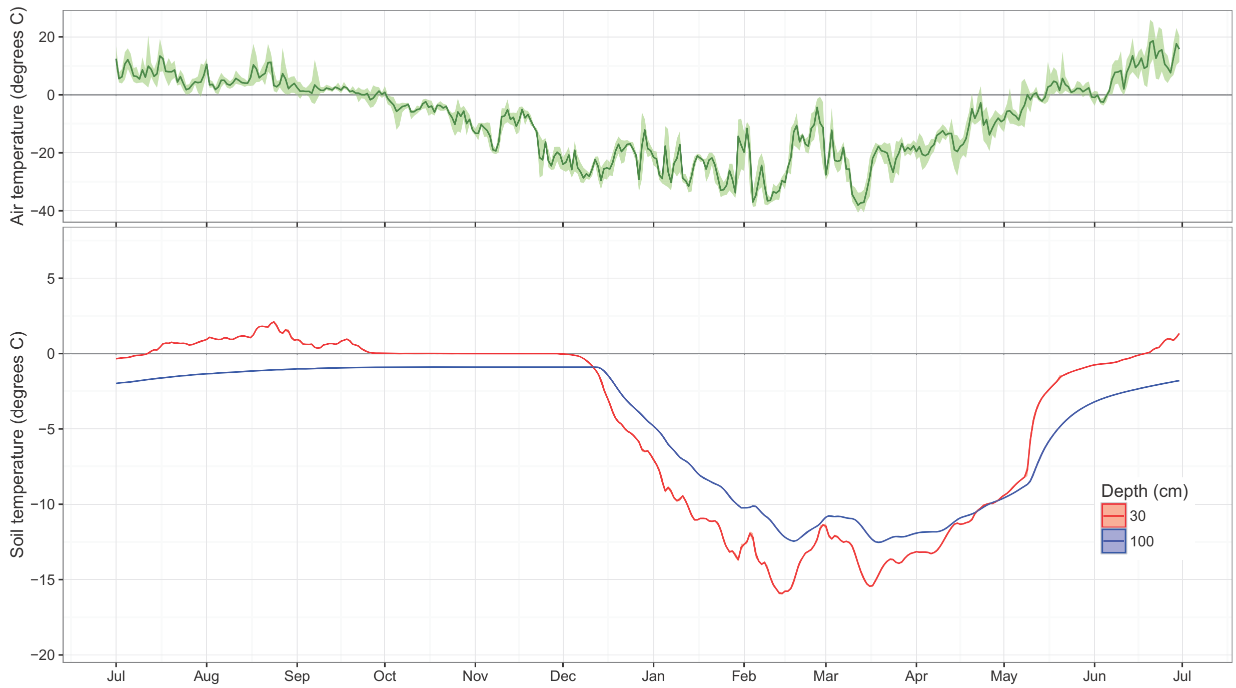

Appendix B-15. Time series of daily median soil temperature at 30 cm and 100 cm at Permafrost Monitoring Plot ts-pc13 (hobo serial number 10392134) and average daily air temperature at the Alpine weather station, CD5 Habitat Monitoring Study, northern Alaska, July 2014–June 2015.

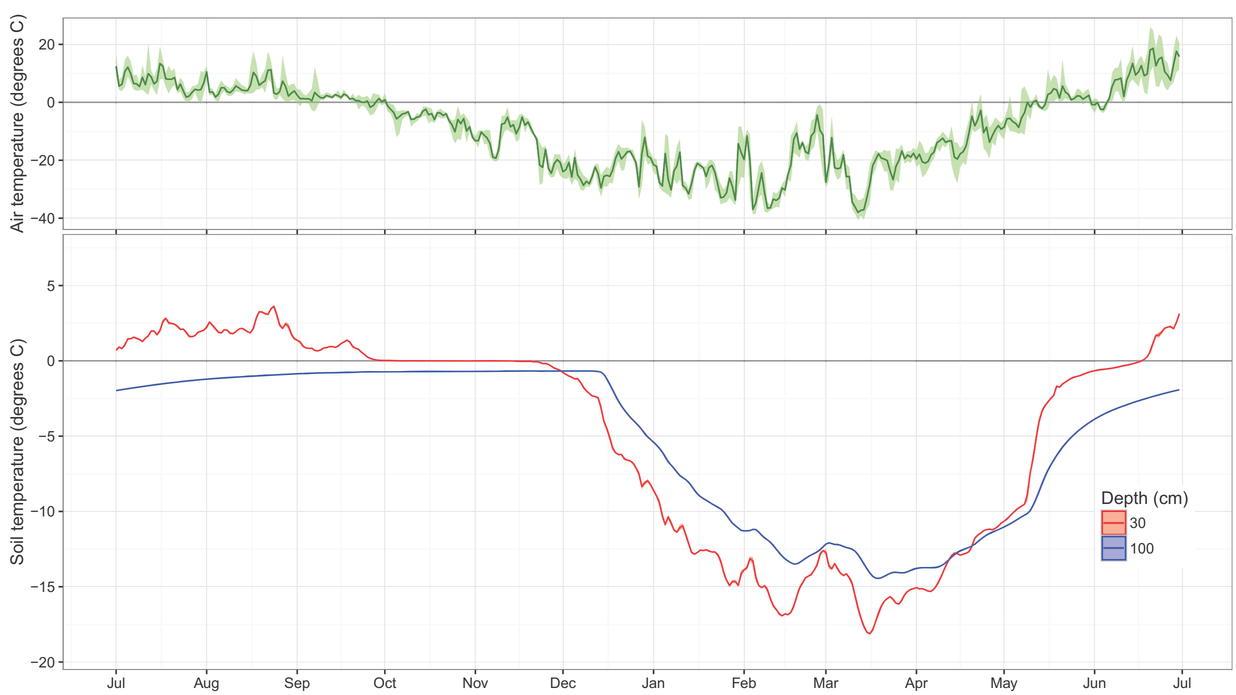

Appendix B-16. Time series of daily median soil temperature at 30 cm and 100 cm at Permafrost Monitoring Plot ts-pc14 (hobo serial number 10392135) and average daily air temperature at the Alpine weather station, CD5 Habitat Monitoring Study, northern Alaska, July 2014–June 2015.